

# **Carbon and oxygen isotopic variation in Upper Maastrichtian chalk, Danish Central Graben**

M-10X (Dan Field), E-5X (Tyra SE Field)

Niels H. Schovsbo & Bjørn Buchardt



# **Carbon and oxygen isotopic variation in Upper Maastrichtian chalk, Danish Central Graben**

M-10X (Dan Field), E-5X (Tyra SE Field)

A contribution to EFP-2001 (1313/01-0001)

Niels H. Schovsbo & Bjørn Buchardt

# Contents

<b>Abstract</b>	<b>4</b>
<b>Introduction</b>	<b>5</b>
<b>Previous work</b>	<b>6</b>
<b>Samples</b>	<b>7</b>
<b>Analytical methods</b>	<b>8</b>
<b>Results</b>	<b>9</b>
Data .....	9
Detailed section in the M-10X well .....	10
Stratigraphic variation of $\delta^{13}\text{C}$ and $\delta^{18}\text{O}$ values .....	10
Chemostratigraphic correlation .....	11
<b>Interpretation</b>	<b>13</b>
Diagenesis .....	13
The detailed sample interval in the M-10X well .....	14
Variation in $\delta^{13}\text{C}$ values .....	14
Variation in $\delta^{18}\text{O}$ values .....	15
Chemostratigraphic correlation .....	15
Estimate of short-term variability of the $\delta^{13}\text{C}$ values .....	15
Chemostratigraphic units and biostratigraphic ties .....	16
Lateral $\delta^{13}\text{C}$ variations .....	16
<b>Implications</b>	<b>18</b>
<b>Chemostratigraphic potential of the <math>\delta^{13}\text{C}</math> variation</b>	<b>20</b>
Comparison with Stevns Klint composite section .....	20
Comparison with other wells from the North Sea .....	20
<b>Conclusions</b>	<b>22</b>
<b>References</b>	<b>23</b>
<b>Table 1</b>	<b>26</b>
<b>Table 2</b>	<b>31</b>
<b>Table 3</b>	<b>32</b>
<b>GEUS</b>	<b>3</b>

## Abstract

The chemostratigraphic potential of the carbon isotopic variation in Upper Maastrichtian chalk has been evaluated based on 143 bulk chalk samples from the M-10X and E-5X wells. The wells are situated 30 km apart and are located in the Dan and Tyra SE oil and gas fields, respectively. Samples were taken each metre to record the stratigraphic variation. In addition, an interval in the M-10X well was sampled on a decimetre scale to resolve the link between  $\delta^{13}\text{C}$ - and  $\delta^{18}\text{O}$ -isotopic variation and lithology.

Across three laminated to bioturbated chalk cycles, the m-scale variation in  $\delta^{13}\text{C}$  is 0.1 ‰. In the middle cycle, more negative  $\delta^{13}\text{C}$  values were measured in the laminated chalk compared to bioturbated chalk. These more negative  $\delta^{13}\text{C}$  values are interpreted to reflect early diagenetic cement characterised by light  $\delta^{13}\text{C}$  values that formed as a response to a semi-closed pore-water environment. No consistent trend was observed in the other cycles. The laminated interval is here weakly developed and possibly reflects a depositional environment characterised by a more open pore-water system that did not allow a diagenetic component to form. The m-scale variation in  $\delta^{18}\text{O}$  values amounts to 0.5 ‰ and shows no apparent relationship to lithology.

A chemostratigraphic correlation between the wells is presented. The correlation is consistent with the established biostratigraphy based on nannofossils, pelagic foraminifers and dinoflagellates. The chemostratigraphy was established based on the m-scale variation in  $\delta^{13}\text{C}$  values and consists of seven units; the chemostratigraphy thus allows a high degree of stratigraphical resolution in the uppermost Maastrichtian interval. Moreover, the combined chemo- and biostratigraphic framework confirms the stratigraphic significance of the log-based porosity markers that form the basis of the cyclostratigraphic correlation system proposed by Toft *et al.* (1996).

The recorded  $\delta^{13}\text{C}$  variation is interpreted to reflect a combination of chalk provenance and seawater signal recorded by settling of pelagic organisms. The local component interpreted to reflect resedimented chalk results in a lateral variability in isotopic composition that, however, does not override the stratigraphical variation. A local component is also evident in the  $\delta^{18}\text{O}$  variation. This component is currently unexplained but is envisioned to reflect differences in fluid flow regime, notably influenced by the timing of hydrocarbon migration.

Comparison with other wells in the Dan and Tyra Fields reveal that the Upper and Lower Maastrichtian chalk have distinctly different stratigraphic  $\delta^{13}\text{C}$  isotopic expressions. This feature clearly suggests that the  $\delta^{13}\text{C}$  variation provides an additional and robust tool in well correlation.

# Introduction

In the Cretaceous Period, carbon isotope stratigraphy has been successfully applied as a correlation parameter and has provided a proxy of the climatic evolution (e.g. Scholle 1977; Scholle & Arthur 1980; Schönfeld *et al.* 1991; Jenkyns *et al.* 1994; Barrera & Savin 1999; Li & Keller 1999; Jarvis *et al.* 2002; Stüben *et al.* 2003; Hart *et al.* 2004). In Denmark, the Upper Cretaceous Chalk Group (Deegan & Scull 1977) in the North Sea are uniform deposits consisting almost entirely of fine-grained calcium carbonate derived from coccoliths, foraminifers and other calcareous micro- and nannofossils (Scholle *et al.* 1998). The chalk is characterised by a high content of very pure (<10 % non-carbonate content) low magnesium calcite from primary pelagic organisms which makes carbon isotopes ideal for stratigraphic correlation (Scholle 1977; Scholle & Arthur 1980). Several authors have inferred that the  $\delta^{13}\text{C}$  variation in the North Sea chalk reflect secular changes in the carbon isotopic composition of the seawater (e.g. Toft *et al.* 1996; Scholle *et al.* 1998) although no wells have been correlated by means of their  $\delta^{13}\text{C}$  variation and hence no detailed carbon isotope stratigraphy has yet been established for the Chalk Group. Instead isotope work has been focused on diagenetic aspects of the chalk (e.g. Jørgensen 1987; Dons *et al.* 1995; Scholle *et al.* 1998) leaving the chemostratigraphic potential almost unattended.

One objective of this EFP-project is to examine the potential for establishing a detailed chemostratigraphic correlation between wells based on the stratigraphical  $\delta^{13}\text{C}$  variation. For this purpose, the E-5X and M-10X wells were sampled and measured for their carbon and oxygen isotopic composition at the Geological Institute Stable Isotope Laboratory in Copenhagen. The M-10X and E-5X wells are located in the southern part of the Danish North Sea within the Salt-Dome Province (Figure 1). The chalk facies in the E-5X and M-10X wells are dominated by chalk deposited by settling of pelagic material. Both wells bear little evidence of disturbance by syndepositional tectonic activity and evidence of large-scale redeposition is absent. Within the North Sea lithostratigraphic framework, the investigated wells represent the Upper Maastrichtian chalk unit 5 and the Lower Danian chalk unit 6 following the nomenclature proposed by Lieberkind *et al.* (1982), corresponding to the Tor and Ekofisk Formations as applied regionally in the North Sea (Evans *et al.* 2003). In order to provide tentative isotopic signatures of all Maastrichtian chalk units, carbon isotope data from published and unpublished reports (Jørgensen 1987, 1990; Dons *et al.* 1995) have been included.

## Previous work

The general geological development of the North Sea and related areas have recently been summarized in great detail in the Millennium Atlas (Evans *et al.* 2003) which covers the most recent literature on chalk sedimentology, litho- and biostratigraphic subdivisions together with the general basin history. Detailed information on the lithologic development including the chalk unit terminology is presented in Lieberkind *et al.* (1982). Detailed studies of the Chalk Group deposits in the Danish North Sea have mainly been focused on the Dan Field (Figure 1). Here studies have been aimed at providing a high resolution timeframe suitable for projecting the field architecture (Lieberkind *et al.* 1982; Schiøler & Wilson 1993; Dons *et al.* 1995; Kristensen *et al.* 1995; Stage 2001; Damholt 2003) and to resolve bed to bed variation in isotopic composition and trace element concentration of the chalk (Scholle *et al.* 1998).

The M-10X well is located on the northern flank of the Dan Field (Figure 1). Isotopic data from the well have previously been presented by Scholle *et al.* (1998) and petrophysical logs have been presented by Kristensen *et al.* (1995) and Toft *et al.* (1996). A dinoflagellate zonation of the well together with other wells from the Dan Field was presented by Schiøler & Wilson (1993) and further interpreted within a seismic stratigraphic framework by Kristensen *et al.* (1995). A study of the sedimentology was presented by Damholt (2003) in a thesis focused on the genesis of the laminated-bioturbated cycles in the Upper Maastrichtian chalk (see also Damholt & Surlyk 2004).

The E-5X well is located on the outer flank of the Tyra SE Field approximately 30 km northwest of the M-10X well (Figure 1). Compared to the M-10X well, the published information from this well is very sparse. Damholt (2003) presented a porosity-based correlation between this well and the M-10X well.

## Samples

Samples for isotopic analysis were selected during the sedimentological logging of the wells (Ineson 2004). The average spacing between the samples is one metre. One section in the M-10X well (the interval from 2015 m to 2017.5 m [6611 to 6620 feet]) was sampled at much greater resolution in order to describe the isotope variability across three cycles composed of laminated to bioturbated chalk. 23 samples were taken here with an average spacing between samples of approximately 12 cm.

Approximately 7 by 7 cm core pieces were picked from the cores at each sample level. From these samples, spot sampling were performed using micro-drilling equipment at the isotope laboratory. Each spot sample consists of approximately 100 mg of carbonate powder drilled from three points within 2 cm distance to each other. Wherever possible, the samples were oriented and drilled parallel to the bedding plane. Laminated to weakly bioturbated chalk was favoured during micro-drilling whereas parts showing evidence of post-depositional changes (i.e. fracture filling, stylolite surfaces) were avoided. In some cases, additional sample material was drilled from a specific core piece using the same procedure as outlined above. These additional samples are labelled with sample number plus 'sub sample 2' in Table 1.

## Analytical methods

The powder spot samples were assigned laboratory numbers and processed at the Geological Institute Stable Isotope Laboratory. Samples were extracted with dichloromethane in order to remove any hydrocarbons present in the rock matrix. For each sample run, 5 mg chalk powder was prepared on an offline isotope preparation system in accordance with the method described by McCrea (1950). The sample was dissolved in vacuum in 100% phosphoric acid at 50 °C. The evolved CO<sub>2</sub> from each sample was filled on an ampoule and carbon and oxygen isotope ratios were measured on a Micromass Isoprime spectrometer.

Corrections for mass spectrometer drift during analysis were done by preparing and running internal working standards for every 10 unknown sample runs. Splits of the LEO working standard were used for working standard as has been the custom at the laboratory since 1981 (Buchardt 2001). Results are reported as ‰-deviations from the V-PDB (Vienna-Pee Dee Belemnite) standard using the  $\delta$ -function defined as:

$$\delta = ((R_{\text{sample}} - R_{\text{standard}}) / R_{\text{standard}}) \times 1000 \text{ ‰}$$

where R is the ratio between the isotope ratio in the sample and the isotope ratio in the standard gas.

Overall reproducibility for carbon and oxygen isotope analysis at the isotope laboratory is better than  $\pm 0.05 \text{ ‰}$  for  $\delta^{18}\text{O}$  and  $\pm 0.03 \text{ ‰}$  for  $\delta^{13}\text{C}$  expressed as  $\pm\sigma$  (standard deviation) for 10 identical samples.

Comparison with the international NBS19 standard is made between repeated analyses of the international standard and the LEO working standard. Due to introduction of the international V-PDB-scale for reporting  $\delta^{13}\text{C}$  and  $\delta^{18}\text{O}$  values, which replaces the older PDB-scale, re-definition of the LEO working standard at the stable isotope laboratory has been applied since 2000. This calibration places the LEO working standard at 1.93 ‰ on the  $\delta^{13}\text{C}$  V-PDB-scale and at -1.96 ‰ on the  $\delta^{18}\text{O}$  V-PDB-scale. Prior calibrations of the LEO working standard placed it at 2.28 ‰ on the  $\delta^{13}\text{C}$  PDB-scale and at -2.04 ‰ on the  $\delta^{18}\text{O}$  PDB-scale (Buchardt 2001).



## Results

All depth measurements reported here refer to core depth (Table 1). Metric measurements used here are calculated from reported depth provided in English feet and inches. For comparison to log depth, 5 feet must be added to the core depth in order to convert these to log depth for both wells. The conversion values were established by comparing the depth of the characteristic log signature of the Cretaceous/Danian hardground visible in the petrophysical logs with the depth of the same interval in the wells (Ineson 2004).

Apart from this isotope study, detailed biostratigraphic and sedimentological studies have been performed by other participants in the project (Ineson 2004; Lassen & Rasmussen 2004; Schiøler, 2004; Sheldon, 2004). The biostratigraphic studies included analysis of nanofossils, benthic and pelagic foraminifers and dinoflagellates in the wells. In order to evaluate the age significance of the isotopic variability presented here, the resulting biostratigraphy (Table 2, see also Ineson *et al.* 2004) and lithological observations have been included here as lithological logs shown on some of the illustrations presented here.

## Data

A total of 165 carbon and oxygen isotope analyses were produced. The data are presented in Table 1 and include analysis of 143 samples, whereof four samples were measured in duplicate. Re-sampling was performed in four cases.  $\delta^{13}\text{C}$  and  $\delta^{18}\text{O}$  measurements of 14 LEO working standards that were prepared and analysed in sequence with the chalk samples are also provided in Table 1.

The  $\delta^{13}\text{C}$  and  $\delta^{18}\text{O}$  values obtained from measurement of the LEO working standard were used in the final data corrections according to Buchardt (2001). The LEO working standard show an internal reproducibility (Table 1) which is within the expected overall reproducibility of the analytical methods ( $\pm 0.05$  ‰ for  $\delta^{18}\text{O}$  and  $\pm 0.03$  ‰ for  $\delta^{13}\text{C}$ ). Reproducibility of the duplicate samples also lies within the uncertainty expressed by the LEO working standard (Table 1 and Figure 2).

In four cases, an additional spot sample was drilled from the same sample. These four sample pairs were not reproduced with the same level of reproducibility as the duplicate samples (Figure 2). The ‰ difference between these sample pairs varies from 0.01 to 0.05 ‰ for  $\delta^{13}\text{C}$  and from 0.05 to 0.1 ‰ for  $\delta^{18}\text{O}$  (Table 1, Figure 2). This suggests that individual spot samples may be significantly different and thus that the reported values are not necessarily representative for the whole sample. This may be of importance when comparing with datasets which have used other sample strategies (i.e. larger samples) and hence obtained values reflecting a broader range of lithologic types present in a single sample.

## Detailed section in the M-10X well

In order to evaluate the short-term (m-scale) variation, a total of 23 additional samples were picked in a ~ 2.5 m thick interval in the M-10X well (Figure 3). The interval is located in the lower part of the cored interval in the well and is part of the cyclic chalk interval characterised by rhythmic alternations in the degree of lamination. The cyclic interval stretches from the base of the well to 1990 m in the M-10X well (Figure 4). The upper part of the well (1990 to 1963 m) does not exhibit these bioturbation-lamination cycles to any significant degree.

The investigated interval contains three laminated-bioturbated cycles (*sensu* Scholle *et al.* 1998; Damholt 2003; Damholt & Surlyk 2004). The lowest laminated-bioturbated cycle (termed Lam-bio cycle 1 on Figure 3) is 1 m thick (2017.4 m to 2016.4 m), the middle cycle (termed Lam-bio cycle 2 on Figure 3) is 0.8 m thick (2015.7 m to 2014.9 m) and the upper cycle (termed Lam-bio cycle 3 on Figure 3) is 0.7 m thick (2016.4 m to 2015.7 m). Within the sedimentological cycles, the bioturbated part may locally display lamination in thin units less than a centimetre thick (Figure 3). The laminated part of the lower cycle exhibits diffuse laminations and shows local signs of bioturbation whereas the laminated chalk in the middle cycle appears devoid of bioturbation and has a better defined lamination (Figure 3). The laminated part of the upper cycle is poorly defined. The lower laminated to bioturbated cycle has a relative low density of stylolites in comparison to the middle and upper cycles, where stylolites occur abundantly in both the laminated and bioturbated chalk (Figure 3).

The  $\delta^{13}\text{C}$  values range between 1.7 ‰ and 1.8 ‰ (i.e. within a range of 0.1 ‰). The base of the middle cycle is marked by a shift in isotopic composition of approximately 0.1 ‰ towards more negative values whereas a gradual return to more positive  $\delta^{13}\text{C}$  values occurs in the bioturbated part of the cycle (Figure 3). In the lower cycle, a 0.1 ‰ shift towards more negative values is observed just below the base of the laminated interval. A few centimetres above the base of the laminated chalk, more positive values are observed. From here and in the upper bioturbated part of the cycle, stable carbon isotopic values are observed (Figure 3).

The  $\delta^{18}\text{O}$  variation shows no obvious relationship with the laminated to bioturbated cycles (Figure 3). The samples vary from -4.6 ‰ to -4.1 ‰ i.e. approximately  $\pm 0.25$  ‰ which may be taken as an estimate of the short-term (m-scale) variation.

## Stratigraphic variation of $\delta^{13}\text{C}$ and $\delta^{18}\text{O}$ values

In both wells, the stratigraphic  $\delta^{13}\text{C}$  variation exhibits an overall decreasing tendency. The decreasing stratigraphic trend in  $\delta^{13}\text{C}$  values is not uniform, however, but occurs in steps, some of which also exhibit subordinate increasing stratigraphic trends (Figure 4). In the E-5X well, values  $>1.75$  ‰ are measured in the lowermost parts of the cored section. From here the  $\delta^{13}\text{C}$  composition decreases to a local minimum at -2100 m where values of 1.55 ‰ are reached. Above this level, the  $\delta^{13}\text{C}$  values increase slightly to 1.75 ‰ measured at 2090 m. Stable values are located from this level and up to 2083 m. Towards the Cretaceous/Danian unconformity, decreasing  $\delta^{13}\text{C}$  values are observed. The sample measured just below the unconformity and the lowermost Danian sample record a 0.2 ‰ shift towards more positive

$\delta^{13}\text{C}$  compositions. In the Danian, an abrupt 0.5 ‰ decrease in isotopic composition is observed (Figure 4).

In the M-10X well, a gradual decrease in  $\delta^{13}\text{C}$  values from 1.9 ‰ at the base of the well to 1.25 ‰ measured at 1988 m is observed. From this level, the  $\delta^{13}\text{C}$  values increase slightly and define a stable trend characterised by near constant values of 1.55 ‰. This value is recorded between 1982 m and 1976 m. At 1976 m, the  $\delta^{13}\text{C}$  composition decreases to 1.25 ‰ in the uppermost part of the Maastrichtian (Figure 4). As in the E-5X well, the uppermost Maastrichtian sample together with the lowermost Danian sample record a 0.2 ‰ shift towards more positive  $\delta^{13}\text{C}$  values (Figure 4). In the Danian, a rapid 0.5 ‰ decrease is also noted. In the uppermost part of the sampled Danian section,  $\delta^{13}\text{C}$  values of about 0.75 ‰ are observed.

The  $\delta^{18}\text{O}$  variation in the E-5X well ranges between -4.0 ‰ to -3.2 ‰ within the Maastrichtian interval, apart from the interval from 2100 m to 2090 m, where the  $\delta^{18}\text{O}$  values increase from -3.3 ‰ to approximately -2.9 ‰. Above this interval, the  $\delta^{18}\text{O}$  values return to the same level as seen in the basal part of the cored section (Figure 5). The range in  $\delta^{18}\text{O}$  values from the M-10X well lies between -5.0 ‰ to -4.0 ‰ and thus only displays limited overlap in  $\delta^{18}\text{O}$  values with the samples from the E-5X well (Figure 6). Across the Cretaceous/Danian unconformity, a 1.5 ‰ increase is noted in both wells. In the Danian, the isotopic ratio decreases to levels seen in the Maastrichtian (Figure 5).

## Chemostratigraphic correlation

The  $\delta^{13}\text{C}$  variation in the M-10X and E-5X wells exhibits a striking overall resemblance (Figure 4). Prominent features include a change from a stable stratigraphical trend to a decreasing stratigraphical trend located in the UC20b nannofossil Zone, a local minimum in  $\delta^{13}\text{C}$  values in the UC20c nannofossil Zone and a local maximum developed in the UC20d nannofossil Zone (Figure 4) that may serve as a chemostratigraphic ties. Another obvious correlation level between the two wells is located in the uppermost part of the wells. Here a stratigraphic decreasing trend in  $\delta^{13}\text{C}$  values reverts to a rapid increase in isotopic composition of 0.2 ‰. The increase in  $\delta^{13}\text{C}$  values do not exactly correspond to the lithologically defined Maastrichtian-Danian boundary developed in the wells as a distinct hardground (see detailed lithological description of the wells presented in Ineson 2004). The abrupt increase in  $\delta^{13}\text{C}$  values occurs in the uppermost Maastrichtian samples picked just below the unconformity in both wells (Table 3). Since the faunal analysis of the chalk in this interval records a mixed Danian-Maastrichtian fauna (Sheldon 2004; Lassen & Rasmussen 2004), the noted increase in  $\delta^{13}\text{C}$  values are interpreted to reflect analysis of Danian sediment that filled burrow systems in the hardground surface. Hence the Maastrichtian/Danian boundary as defined from geochemistry is located below the boundary as defined from lithology.

In order to evaluate the stratigraphic variation further, the short-term (m-scale) variability of 0.1 ‰ established from Figure 3 is used to construct a data envelope (Figure 7). From evaluation of the data envelope, the curves are divided into 'units' with characteristic trends in the data variation. The boundaries between each 'unit' then subsequently serve as correlation horizons. The result of this produces a correlation which focuses on local or absolute maxima, minima and curve inflection points. The benefit of this graphic approach is that in-

formation on the short term variability of the data can be integrated directly into the analysis. Enhancing the short term variability generally leads to broader envelopes with less characteristic bends.

By applying this method, the stratigraphical  $\delta^{13}\text{C}$  variation in the M-10X well is broken down into seven units termed, A – G (Figure 7). In a similar manner, the stratigraphic  $\delta^{13}\text{C}$  variation in the E-5X well results in a subdivision of the cored interval into 5 units. The depth intervals of the units are presented in Table 3 and a brief description of the units A – G follows below:

Unit A:

Decreasing  $\delta^{13}\text{C}$  values (0.2 ‰) located in the uppermost part of the UC20d nannofossil Zone.

Unit B:

Stable  $\delta^{13}\text{C}$  values in the middle part of the UC20d nannofossil Zone. In the E-5X well the base of this unit is unconstrained due to poor recovery. In the M-10X well, the boundary to the above-lying A unit is marked by a shift towards more positive values. This feature is not observed in the E-5X well.

Unit C:

Increasing  $\delta^{13}\text{C}$  values (0.2 ‰) located in the UC20c nannofossil Zone extending into the lowermost part of the UC20d nannofossil Zone. The increase approximates to 0.2 ‰ in the E-5X well, whereas the increase is smaller in the M-10X well.

Unit D:

Decreasing  $\delta^{13}\text{C}$  values (0.2 ‰) located in the upper part of the UC20b nannofossil Zone extending to the lower part of the UC20c nannofossil Zone.

Unit E:

Stable  $\delta^{13}\text{C}$  values in the middle part of the UC20b nannofossil Zone.

Unit F (only present in the M-10X well):

A 0.2 ‰ decrease in  $\delta^{13}\text{C}$  values located in the uppermost part of the UC20a nannofossil Zone extending into the lowermost part of the UC20b nannofossil Zone.

Unit G (only present in the M-10X well):

A >0.1 ‰ decrease in  $\delta^{13}\text{C}$  values located in the UC20a nannofossil Zone. The base of this unit is not known.

# Interpretation

## Diagenesis

Calcite in equilibrium with Maastrichtian seawater is expected to lie between -2 and 0 ‰ in  $\delta^{18}\text{O}$  values (e.g. Jørgensen 1987). Recent measurements of the fine-grained chalk fraction from Stevns Klint (Hart *et al.* 2004) confirm this. Here the Upper Maastrichtian interval ranges between -2 and -1.5 ‰ in  $\delta^{18}\text{O}$  values (Figure 8). Indication of cooling periods are seen as intervals where the  $\delta^{18}\text{O}$  values define consistent trends towards less negative  $\delta^{18}\text{O}$  isotopic compositions, as observed in the uppermost part of the Maastrichtian interval (Figure 8).

In the M-10X and E-5X wells, the measured  $\delta^{18}\text{O}$  values range between -3 ‰ and -5 ‰ (Figure 5). Covariance in  $\delta^{18}\text{O}$  values between the M-10X and E-5X wells is noted, particularly in the upper part of the Maastrichtian interval (Figure 9). Notable features include less negative  $\delta^{18}\text{O}$  values in the uppermost part of unit B and possibly also across the C/B unit boundary (note that this boundary interval in the E-5X well is poorly identified due to core loss). Since the  $\delta^{18}\text{O}$  values are several ‰ more negative than those measured at Stevns Klint (Figure 8), the observed covariance between the wells cannot safely be interpreted to reflect a primary signature without supporting evidence. In the M-10X well, the m-scale variation in  $\delta^{18}\text{O}$  values was estimated to be 0.5 ‰ (Figure 3). At Stevns Klint, the m-scale variation in  $\delta^{18}\text{O}$  values is less than 0.5 ‰, as seen by the fitted 0.5 ‰ envelope in Figure 8. The broader range in isotopic compositions in the North Sea is also likely to reflect a diagenetic overprint of the primary variation.

The effect on the  $\delta^{18}\text{O}$  isotopic composition during diagenesis has been the subject of numerous studies (e.g. Scholle 1977; Jørgensen 1987; Dons *et al.* 1995; Scholle *et al.* 1998). The general notion is that shifts in  $\delta^{18}\text{O}$  composition towards negative isotopic compositions reflects isotopic exchange at elevated temperatures between carbonate and pore-water in a closed rock-fluid system. In contrast to the  $\delta^{18}\text{O}$  variation, the  $\delta^{13}\text{C}$  variation is generally believed to retain its primary variation better due to the rock-dominated nature of the diagenesis (e.g. Jørgensen 1987; Scholle *et al.* 1998).

In Figure 6, the carbon and oxygen isotope composition does not exhibit any clear correlation. The variation in Figure 6 is thus in good agreement with the above-cited authors indicating that the  $\delta^{18}\text{O}$  isotopic composition has been significantly affected by burial diagenesis in contrast to the  $\delta^{13}\text{C}$  isotopic compositions. The most profound feature in the  $\delta^{18}\text{O}$  variation in Figure 6 is that the samples from the two wells do not plot within the same range in  $\delta^{18}\text{O}$  values. Hence the vast majority of the samples from the M-10X well are characterised by  $\delta^{18}\text{O}$  values below -4 ‰ whereas samples from the E-5X well have  $\delta^{18}\text{O}$  values above -4 ‰. This feature in Figure 6 appears to be related to a geographic difference in  $\delta^{18}\text{O}$  values in the North Sea and has been documented to some extent by Jørgensen (1987). Although a detailed account of the possible reasons for this feature is beyond the scope of this paper it can be inferred that the geographic differences are apparently related to the overall burial

history including regional differences in fluid conditions. At a basin scale, differences in fluid conditions, e.g. temperature, salinity and fluid movements including displacement of pore-water with hydrocarbons, are all known variables (Evans *et al.* 2003).

## The detailed sample interval in the M-10X well

### Variation in $\delta^{13}\text{C}$ values

In a study from the Dan Field, Scholle *et al.* (1998) observed a tendency for laminated chalk samples to have slightly more negative  $\delta^{13}\text{C}$  values compared to bioturbated chalk samples. Scholle *et al.* (1998) were not, however, able to document this feature since the statistical separation between the groupings was too low.

Of the lithologically defined cycles, only the middle cycle displayed a systematic relationship between lithology and  $\delta^{13}\text{C}$  variation (Figure 3). Here more negative  $\delta^{13}\text{C}$  values were measured in the laminated part whereas the bioturbated part was characterised by more positive values. According to Scholle *et al.* (1998), the laminated samples might be expected to have received a higher proportion of isotopically light cement derived from  $\text{CO}_2$  that was produced from re-oxidation of organic matter. Hence the isotope signature was not derived from the water column but is an overprint formed in the sediment due to a specific early diagenetic environment. The return to more positive values in the bioturbated intervals reflects venting of the pore waters by infaunal organisms which prevented a special diagenetic signature precipitating from the pore-water.

The isotopic variation in the lower and upper cycles does not show any relationship with lithology (Figure 3). This might be ascribed to the weak lamination and sporadic signs of bioturbation. These features might suggest that the depositional environment was characterised by a more open pore-water system such that cement with light  $\delta^{13}\text{C}$  isotope compositions did not form in sufficient quantities to affect the whole rock isotopic signature. Hence, it is assumed that only minor differences in the degree of bioturbation and thus openness of the pore-water system have a significant on the isotope signature.

The laminated lithofacies have been interpreted to reflect either anoxic to dysoxic bottom water conditions (Damholt 2003; Damholt & Surlyk 2004) or high sedimentation rates (Scholle *et al.* 1998). The isotopic signature discussed above can result from either of the scenarios and hence does not bring any new conclusive evidence to this debate. The reason for this is that the geochemical signature is interpreted to reflect a poorly vented pore-water system in which isotopically light cement formed as a consequence of organic matter remineralization. Such an environment might result from anoxic conditions at the seafloor, which prevented an infaunal community from developing according to Damholt (2003) and Damholt & Surlyk (2004), or might be the result of fast sedimentation events that sealed off the pore-water system by adding a thick pile of sediments, as postulated by Scholle *et al.* (1998).

## Variation in $\delta^{18}\text{O}$ values

Scholle *et al.* (1998) documented that laminated chalk is approximately 0.3 ‰ more negative in  $\delta^{18}\text{O}$  values compared to bioturbated chalk. They ascribed this finding to differences in early seafloor cementation. Thus, bioturbated chalk received a higher proportion of seafloor cement whereas laminated parts were left relatively uncemented after early diagenesis. The isotopic difference developed later since larger quantities of isotopically light  $\delta^{18}\text{O}$  cement formed in the chalk with less early diagenetic cement (Scholle *et al.* 1998).

The  $\delta^{18}\text{O}$  signature of the different lithotypes reported by Scholle *et al.* (1998) cannot be confirmed in the present study since the majority of the samples plot within a range of 0.5 ‰ regardless of lithology (Figure 3). A slight tendency to higher sample-to-sample variation is, however, noted in the bioturbated parts of each of the laminated-bioturbated cycles, potentially reflecting minor differences in early seafloor cementation. The lack of a systematic relationship between  $\delta^{18}\text{O}$  variation and lithology is, however, not unexpected according to Scholle *et al.* (1998) since they altogether examined three pairs of laminated to bioturbated cycles and only found the above-described relationship in one case. The fact that the relationship between  $\delta^{18}\text{O}$  values and lithology is apparently rare might suggest that the impact of differential sea-floor cementation followed by differential addition of burial cement on the  $\delta^{18}\text{O}$  variation proposed by Scholle *et al.* (1998) cannot be safely deduced from the lithology alone.

## Chemostratigraphic correlation

### Estimate of short-term variability of the $\delta^{13}\text{C}$ values

In the M-10X well, the cyclic chalk interval is developed from the base of the cored section in the well and up to 1990 m; above this level laminated-bioturbated cycles are scarce (Ineson 2004; Figure 7). In the non-cyclic interval, only scattered occurrences of weakly laminated chalk are observed in the upper part of the well (e.g. Figure 7). In comparison, the E-5X well only displays weakly developed laminated-bioturbated cycles in the same stratigraphic intervals (Figure 7). Only the interval between 2100 and 2110 m shows a poorly developed laminated-bioturbated cyclicity. In the remainder of the well, lamination is rare and the cored interval is generally characterised by bioturbated chalk (Ineson 2004).

For both wells, the m-scale range of 0.1 ‰ adopted from Figure 3 appears to be a good estimate of the m-scale variation, regardless of the lithological development (Figure 7). This range in  $\delta^{13}\text{C}$  values was used to construct the data envelope and hence is an integrated part of the chemostratigraphy presented in Figure 7. If the range is too large, then fewer chemostratigraphic ties can be established. Since the estimate of the short-term variability is based on the isotopic variability in a cyclic chalk interval, it might be expected that this variation is too high for non-cyclic chalk sequences since cement with light  $\delta^{13}\text{C}$  isotopic signature would not be expected to form here. Since no detailed sections were sampled through non-cyclic chalk, no adjustment of the short-term range can be made at present even though the estimate is probably too high for some intervals.

## Chemostratigraphic units and biostratigraphic ties

The biostratigraphic framework established for the two wells is based on nannofossils, pelagic foraminifers and dinoflagellates and allows a test of the validity of some of the boundaries between the chemostratigraphic units (Figures 10 and 11). The boundaries between the B/C, C/D and D/E units are well-constrained biostratigraphically, whereas in the uppermost part of the Maastrichtian (units A and B) and in the basal part of the cored section (units F and G) no biostratigraphic ties are available. Since the units do not conflict with known biostratigraphy, they are assumed to represent isochronous units. In the uppermost part of the Maastrichtian and in the lower cored interval, the chemostratigraphy even provides a higher stratigraphic resolution than the biostratigraphy (Figure 10).

The consistency between the boundaries based on chemostratigraphy and biostratigraphy can be tested by examining the relative depth of the boundaries between the wells (Figure 11). This picture reveals a rather smooth thickness relationship suggesting that the areas accumulated comparable thicknesses of chalk during each of time steps. The largest deviation from this trend is seen within the interval spanning the uppermost part of unit D and the lowermost part of unit C (Figure 11). Here the thickness of the uppermost part of the D unit is thicker in the E-5X well than in the M-10X well whereas the lowermost part of the C unit in the M-10X well is thicker than the same interval in the E-5X well. The thickness variation suggests either that local differences in sedimentation occurred at this time or that the exact position of the boundaries can be questioned.

The boundary between the D and C units is constrained by the boundary between the FCS23a/b foraminifer Zones. In both wells, this boundary is positioned just above the D/C unit boundary. The precise location of the FCS23a/b boundary proved, however, to be problematic in the wells (Lassen & Rasmussen 2004). If the FCS23a/b boundary is removed then the boundary between the D and C units is unconstrained and could potentially have been slightly misplaced. The boundary between the D and C units corresponds to a local minimum in the stratigraphic variation of the  $\delta^{13}\text{C}$  values (Figure 7). In the E-5X well, this level is well expressed. In the M-10X well, however, the local minimum was picked corresponding to a level where a sample plots off-trend towards more negative carbon isotopic compositions compared to the other samples (Figure 7). If this sample (measured in duplicate) is removed from the evaluation of the shape of the curve, then the curve minima and hence the boundary between the D/C units should be positioned at 1984m (6510 feet) in the well. If this level is chosen, then the thickness variation of the D and C units between the wells is minor.

## Lateral $\delta^{13}\text{C}$ variations

The above example of difficulties in establishing the D and C unit boundary in the M-10X well clearly illustrates that local conditions affect the  $\delta^{13}\text{C}$  variation. Because the correlation based on chemostratigraphy is in general agreement with the biostratigraphy it appears that the general secular nature of the  $\delta^{13}\text{C}$  variation is not in doubt.

The local component that creates difficulties in locating the D and C unit boundary can be described as a tendency for samples from the M-10X well to have more negative  $\delta^{13}\text{C}$  compositions than time-equivalent samples from the E-5X well. The offset in  $\delta^{13}\text{C}$  values is es-



pecially evident for samples belonging to the C unit where the samples from the two wells differ by up to 0.2 ‰ (e.g. Figure 7).

In a  $\delta^{13}\text{C}$  versus  $\delta^{18}\text{O}$  diagram, unit C samples define a linear correlation that might suggest that the difference in  $\delta^{13}\text{C}$  values is related to the difference in  $\delta^{18}\text{O}$  values between the wells (Figure 12). The difference in  $\delta^{18}\text{O}$  values between the wells was related to basin-scale differences in fluid dynamics (see above) although no detailed account was provided. Hence it is difficult to evaluate whether the linear relationship displayed by the samples from the C unit in Figure 12 reflects a combined response to a presumed late diagenetic cause or whether the two components (i.e. lowering of the  $\delta^{13}\text{C}$  values and lowering of the  $\delta^{18}\text{O}$  values in the M-10X well compared to the E-5X well) are independent variables.

The statistically significant correlation displayed between  $\delta^{13}\text{C}$  and  $\delta^{18}\text{O}$  values is a feature restricted to the C unit since samples from unit D do not exhibit any statistically significant (>90% level) correlation (Figure 12). It should be noted that the possible shift in the position of the boundary between the C and D in the M-10X well discussed above and indicated in Figure 10 does not affect the statistically significant correlation between the C unit samples or the lack of correlation observed between the samples from the D unit (Figure 12).

The stratigraphic variation of  $\delta^{13}\text{C}$  and  $\delta^{18}\text{O}$  values in the C unit from the M-10X well indicate that rapid shifts in  $\delta^{18}\text{O}$  values were not counterbalanced by changes in  $\delta^{13}\text{C}$  values, as might be expected from Figure 12. This can be seen in the M-10X well where samples analysed across the firmground interval (1980 to 1982m) exhibit 2 ‰ variations in  $\delta^{18}\text{O}$  values (Figure 9). In the same interval, the  $\delta^{13}\text{C}$  values do not differ significantly (Figure 7). If the variations in  $\delta^{18}\text{O}$  values reflect local differences in burial diagenesis then this process apparently did not alter the  $\delta^{13}\text{C}$  composition. Hence the  $\delta^{13}\text{C}$  values are largely unaffected by burial diagenesis. Other studies have also shown that the  $\delta^{13}\text{C}$  composition does not correlate with the amount of microspar present as intergranular secondary cement in the chalk, in contrast to the  $\delta^{18}\text{O}$  values (Jørgensen 1987) suggesting that the  $\delta^{13}\text{C}$  variation is not controlled by the presence of a specific cement type.

Instead, the differences in  $\delta^{13}\text{C}$  values between the wells are interpreted to reflect a primary feature. Such a difference may reflect local differences in the faunal composition of the chalk. This effect may arise both from a 'vital effect' that describes the species dependant fractionation in  $\delta^{13}\text{C}$  values during formation of calcite in the water column or result from depth-related differences in  $\delta^{13}\text{C}$  values of the seawater. As a consequence of this, chalk with a high proportion of benthic organisms is expected to display more negative  $\delta^{13}\text{C}$  values compared with chalk with a low content of benthic organisms. Currently, no quantification of the faunas has been made that otherwise would have allowed for an evaluation of this. Instead the main mechanism for the lateral component is envisioned to be different amounts of local allochthonous chalk from sources with variable  $\delta^{13}\text{C}$  isotopic signatures. Apparently the influence of this component varied in time and was more profoundly expressed in unit C where it resulted in a 0.2 ‰ difference in the recorded isotopic composition. This component was not as dominant during deposition of unit D since the difference in isotopic composition between the wells is minor (Figure 12).

## Implications

The combined chemo- and biostratigraphic framework can be used to test the cyclostratigraphy proposed by Toft *et al.* (1996). This type of stratigraphy uses characteristic 'peaks' and 'lows' in the porosity logs and is based on reference profiles, including the M-10X well (Toft *et al.* 1996). In this well, Toft *et al.* (1996) identified and labelled 11 marker peaks on the porosity log in the Upper Maastrichtian. Of these, 6 cyclostratigraphic log markers are within the cored interval (Figure 10). In the E-5X well, the log markers have also been identified by Damholt (2003). Of these peaks, the 'b' marker is of special interest since it denotes a distinct high porosity interval which serves as an important reservoir unit in the North Sea (Toft *et al.* 1996).

The cyclostratigraphic markers appear to be located in the chalk in a manner that is consistent with the chemo- and biostratigraphic framework (Figures 10 and 11) and therefore the chronostratigraphic significance of these log markers is confirmed. The cyclostratigraphic log markers do not relate to the chemostratigraphic units in a consistent manner. This suggests that the timing of the characteristic peaks in the porosity log is not linked with changes in the carbon cycle as reflected in the  $\delta^{13}\text{C}$  values. As with the chemostratigraphic units, the cyclostratigraphic log markers do not coincide exactly with any of the biostratigraphically defined boundaries. This relationship is, however, not expected since the biostratigraphically defined boundaries are typically based on appearances or disappearance of one or a few species that only constitute a minor proportion of the fauna/flora. The chemostratigraphic boundaries and the cyclostratigraphic markers may, however, co-vary with larger differences in the faunal composition.

Scholle *et al.* (1998) and Damholt (2003) have both explained the cyclicity in the porosity log as a feature generated by diagenetic processes. According to Scholle *et al.* (1998), the porosity is generated by differences in seafloor cementation created by pulses in sedimentation rate. In contrast, Damholt (2003) held that the cyclicity was forced by redox changes and created by different degrees of bioturbation that affects the packing of the sediment. In this model, the redox changes fluctuate within the Milankovitch frequency band (Damholt & Surlyk 2004) thereby creating an indirect or subordinate relationship between porosity cycles and orbital forcing. Hence one would not anticipate the same type of porosity variation to develop between areas that differ considerably in oxygenation level at the seafloor.

Though both models cannot be correct, it was nevertheless anticipated that the wells would display a higher degree of lithological similarity than that measured (e.g. compare logs in Figure 7, see also Ineson 2004). The reason for this is that both models assume that the porosity variations are controlled by sedimentary processes and hence are related to the chalk facies. Instead, it appears that comparable porosity variations are preserved in time-equivalent chalk that display cyclic laminated-bioturbated facies in one core (M-10X) and non-laminated bioturbated facies in the other (E-5X, Figure 10). The similarity of the porosity cycles in this interval includes not only the consistent locations of the marker peaks but also a striking resemblance in the overall stacking pattern of the cycles. This might suggest that porosity variations are less controlled by conditions on the seafloor than envisioned by Scholle *et al.* (1998) and Damholt (2003). Instead, as noted by Stage (2001), the cyclic

variations at least in part may have been controlled by variations in the detrital influx, driven by climatic variations. Accordingly the variations in porosity may be a reflection of lithological variation in the chalk (i.e. texture, composition) rather than being a reflection of a specific fabric imposed by the depositional environment. The relationship between lithotypes and porosity as documented in great detail by Damholt (2003) in the Dan Field area is striking. The resemblance does not, however, necessarily imply that the relationship between sedimentary facies and porosity variations in this area are directly related since it cannot be ruled out that the relationship is in fact indirect. Such an indirect relationship can be generated if the textural properties of the chalk that leads to the formation of high porosity beds were related to the conditions that promoted laminated lithotypes to form. Adopting this approach, the similarity in porosity logs between the M-10X and E-5X wells becomes less problematic.

# Chemostratigraphic potential of the $\delta^{13}\text{C}$ variation

## Comparison with Stevns Klint composite section

Hart *et al.* (2004) have recently published a detailed carbon isotopic profile through the uppermost Maastrichtian at Stevns Klint (Figure 8). In the profile, the short-term variation noted in the M-10X well has been used to construct isotope units in a similar manner to that presented here for the North Sea wells. At Stevns Klint, three long-term trends in the  $\delta^{13}\text{C}$  variation have been identified (Figure 8). These correspond to two stable intervals (labelled 1 and 2 in Figure 8) separated by a shift in isotopic values and a lower interval characterised by an increasing trend in the  $\delta^{13}\text{C}$  values (labelled 3 in Figure 8).

The Stevns Klint composite section lies within the *P. grallator* dinoflagellate Zone (Pgr). The same interval in the North Sea corresponds to a level within the middle part of unit C (Figure 10). Compared with the North Sea, the Stevns Klint section contains no direct counterpart to the unit A which is characterised by a decreasing trend in the  $\delta^{13}\text{C}$  values. In the North Sea, the A/B unit boundary is characterised by a 0.1 ‰ shift in  $\delta^{13}\text{C}$  values in the M-10X well. Compared to Stevns Klint, this shift may be correlated with the boundary between intervals 1 and 2. Interval 1 thus corresponds to the basal part of unit A and interval 2 at Stevns Klint is interpreted to correspond to the B unit established in the North Sea. The lower interval labelled 3 at Stevns Klint may correspond to the top of unit C that is also characterised by increasing  $\delta^{13}\text{C}$  values.

The above correlation is tentative at present and should be strengthened by applying the subzonation of the Pgr dinoflagellate Zone to the Stevns Klint section as applied to the M-10X well by Schiøler & Wilson (1993). The apparent discrepancy between the uppermost parts of the section would need to be further addressed. The differences in the carbon isotopic variation might be due to a hiatus at Stevns Klint or to be related to different sampling approaches. Hence, it would be advantageous to conduct the analysis upon either only the fine-grained fraction or on foraminifers in the North Sea in order to be able to compare more directly with the data presented by Hart *et al.* (2004).

## Comparison with other wells from the North Sea

The chemostratigraphic units defined here cannot be compared directly to other carbon isotope investigations in the southern part of the Central Graben (e.g. Jørgensen 1987, 1990; Dons *et al.* 1995) due to either low sample density or lack of stratigraphic resolution. However, the data altogether do allow a general reconstruction of the carbon isotopic variation of the Lower Danian to Campanian–?Santonian chalk in the southern Central Graben (Figure 13).

No age model has yet been applied in the presentation of the stratigraphic variance in  $\delta^{13}\text{C}$  values (Figure 13). This implies that the original spacing between the samples has been

maintained and hence no correction for thickness variation of individual biozones between the wells has been done. The fitting of curves was performed by placing the wells in such a manner that the biostratigraphic ties were in agreement, although a slight offset was accepted. As a consequence, the resulting range in  $\delta^{13}\text{C}$  values are approximately 4 times higher than the short term variation noted in Figure 3. Part of the observed range in  $\delta^{13}\text{C}$  values in any given time interval obviously also reflects the lateral component in the  $\delta^{13}\text{C}$  variation.

Despite this, the reconstructed  $\delta^{13}\text{C}$  curve (Figure 13) reveals that the decreasing trend in  $\delta^{13}\text{C}$  values in the Upper Maastrichtian defined by the M-10X, E-5X and MFB-7 wells differs from the Lower Maastrichtian chalk as defined by the M-1X and lower parts of the MFB-7 wells which exhibit a plateau of approximately 2.25 ‰. Consequently, the different curvature expressed by  $\delta^{13}\text{C}$  values appears to be an excellent marker for separation of chalk deposited during Early or Late Maastrichtian time. The general shape of the reconstructed  $\delta^{13}\text{C}$  curve is in good agreement with results gained in other studies (e.g. Jenkyns *et al.* 1994; Barrera & Savin 1999) and is generally considered to be a reflection of secular variation in the carbon isotopic composition of the seawater during the Maastrichtian.

In Figure 13, the lowermost part of the Early Maastrichtian is characterised by a pronounced negative isotope excursion. The negative carbon isotopic excursion (3 ‰) cannot be correlated precisely outside the North Sea area since it has no direct parallel in the Maastrichtian or in the Campanian (e.g. Jarvis *et al.* 2002). In the North Sea, the excursion is also present in the basal part of the Ruth-1 well (see data appendices in Jørgensen, 1990) as well as in the E-4X well (2099 m to 2161 m). In the E-4X well, the excursion corresponds to a change from pure chalk to chalk with clay-rich intervals, judging from the descriptions in the completion report (Chevron 1976). The excursion might also be present in the basal part of the E-2X well where a similar change in lithology appears (see data appendices in Jørgensen, 1990). This particular interval is, however, analysed with too large internal spacing between the samples to allow for a positive identification of the excursion.

It should be noted that the interval in the E-4X well in which the negative carbon isotope excursion occurs is dated to the NUK3-6 nanofossil zone (Barrington 1993) characterised by *Reinhardtites levis*, *Prediscosphaera arkhangel'ski*, *Calculites obscurus*. This level corresponds to the uppermost Lower Maastrichtian according to the zonation scheme presented by Barrington (1993). If the zonation scheme of Barrington (1993) is equivalent to the zonation scheme proposed by Schiøler & Wilson (1993), then the negative carbon isotope excursion in the E-4X well is contemporaneous with the lower part of the M-1X well in which no comparable negative isotope excursion is located (Figure 13). At present, the possibility exists that the negative carbon isotope excursion in the E-4X well and hence the NUK3-6 zones corresponds to the lowermost Early Maastrichtian (or older) according to Schiøler & Wilson (1993). Hence the excursion might be located below the cored interval in the M-1X well and reflects a previously unrecognised 'event'. Alternatively, it represents a more extreme development of the Late Campanian negative carbon isotope excursion as documented by Jarvis *et al.* (2002). The significance of this excursion outside the North Sea area is thus not established and further documentation is needed.

## Conclusions

Seven chemostratigraphic units have been defined in the M-10X and E-5X wells based on the stratigraphic variation in the  $\delta^{13}\text{C}$  values.

The chemostratigraphic units are in agreement with the available biostratigraphy and confirm the chronostratigraphic significance of the cyclostratigraphic markers defined by Toft *et al.* (1996). Moreover, the chemostratigraphic units allow a higher stratigraphic resolution in the uppermost Maastrichtian interval than current biostratigraphy.

Across three bioturbated to laminated chalk cycles, the m-scale variation in  $\delta^{13}\text{C}$  is 0.1 ‰. In the middle cycle, more negative  $\delta^{13}\text{C}$  values were measured in the laminated chalk compared to bioturbated chalk. This signature is interpreted to reflect early diagenetic cement with a light  $\delta^{13}\text{C}$  isotopic signature that formed as a response to a semi-closed pore-water environment. No consistent trend was observed in the lower and upper cycles. The laminated intervals are here more weakly developed and possibly reflect a depositional environment characterised by an open pore-water system that did not allow a diagenetic component to form. The m-scale variation in  $\delta^{18}\text{O}$  values are 0.5 ‰ and show no apparent relationship to lithology.

A lateral component in the  $\delta^{13}\text{C}$  variation has been identified. It is interpreted to reflect lateral differences in the amount of allochthonous chalk with variable  $\delta^{13}\text{C}$  isotopic composition although primary compositional differences in the faunal composition cannot be ruled out. This lateral component does not override the stratigraphic variation. Accordingly, the recorded  $\delta^{13}\text{C}$  variation is interpreted to reflect a combination of chalk provenance and a sea-water signal recorded by settling of pelagic organisms.

A lateral component is also present in the  $\delta^{18}\text{O}$  variation. The M-10X well is shifted 1 ‰ towards lower  $\delta^{18}\text{O}$  values compared to the E-5X well. This component is currently unexplained but is apparently not linked with the lateral  $\delta^{13}\text{C}$  component. Instead it is envisioned to reflect differences in fluid flow regime, notably influenced by the timing of hydrocarbon migration.

Comparison with other wells in the Dan and Tyra SE Fields indicate that the Upper Maastrichtian and Lower Maastrichtian chalks have distinctly different stratigraphic  $\delta^{13}\text{C}$  isotopic expressions. This feature suggests that the  $\delta^{13}\text{C}$  variation provides a robust additional tool for correlation, even in wells with relatively low sample density.

## References

- Barrera, E. & Savin, S., 1999: Evolution of late Campanian–Maastrichtian marine climates and oceans. In Barrera, E. & Johnson, C.C. (Eds): Evolution of the Cretaceous ocean-climate system. Geological Society of America Special Paper **332**, 245–281.
- Barrington, D.I., 1993: A biostratigraphic correlation of the Maastrichtian of the TEB-1P, TEP-12, and Upper Cretaceous of the E-4X, TWC-3P. Report 4862/1a, Simon Petroleum Technology, England, 1–9 (in archives of Geological Survey of Denmark and Greenland, GEUS Report File **3319**).
- Bayliss, D.D., Standring, A.J. & Meyrick, R.W., 1976: E-4X, paleontological/stratigraphical final report – depth 260’-7510’. Paleoservices, England, 1–16 (in archives of Geological Survey of Denmark and Greenland, GEUS Report File **12635**).
- Buchardt, B., 2001: Standard kalibrering november 2000. Stabil isotop laboratoriets interne rapport **2001-1**. Geologisk Institut, Københavns Universitet. 1–6.
- Chevron, 1976: E-4X completion report, (in archives of Geological Survey of Denmark and Greenland, GEUS Report File **4620**).
- Damholt, T., 2003: Cycles in Upper Maastrichtian chalk of the Southern Central Graben, Danish North Sea: formation and chronostratigraphical significance. Unpublished Ph.D. thesis, Faculty of Science, University of Copenhagen, 196 pp.
- Damholt, T. & Surlyk, F., 2004: Laminated–bioturbated cycles in Maastrichtian chalk of the North Sea: oxygenation fluctuations within the Milankovitch frequency band. *Sedimentology* **51**.
- Deegan, C.E. & Scull, B.J., 1977: A proposed standard lithostratigraphical nomenclature for the Central and Northern North Sea. Report of the Institute of Geological Sciences **77/25**; Bulletin of the Norwegian Petroleum Directorate 1.
- Dons, T., Jakobsen, F. & Stentoft, N., 1995: Chalk diagenesis and reservoir properties – Dan Field case study. DGU Service Report **15**, 83 pp-Copenhagen: Ministry of Environment and Energy. Geological Survey of Denmark.
- Evans, D., Graham, C., Armour, A. & Bathurst, P. (editors and co-ordinators), 2003: The Millennium Atlas: petroleum geology of the Central and Northern North Sea. The Geological Society of London. London.
- Hart, M.B., Feist, S.E., Price, G.D. & Leng, M.J., 2004: Reappraisal of the K-T boundary succession at Stevns Klint, Denmark. *Journal of the Geological Society, London* **161**, 885–892.
- Ineson, J.R., 2004: Sedimentology of the Upper Maastrichtian chalk, Danish Central Graben. A contribution to EFP-2001 (1313/01-0001). Danmarks og Grønlands Geologiske Undersøgelse Rapport **2004/89**.
- Ineson, J.R., Buchardt, B., Lassen, S., Rasmussen, J.A., Schovsbo, N.H., Schiøler, P. & Sheldon, E., 2004: Palaeontology, stable isotopes and sedimentology of the Upper Maastrichtian, Danish Central Graben: a record of palaeoclimatic and palaeoceanographic change. A contribution to EFP-2001 (1313/01-0001). Danmarks og Grønlands Geologiske Undersøgelse Rapport **2004/81**.
- Jarvis, I., Mabrouk, A., Moody, R.T.J. & de Cabrera, S., 2002: Late Cretaceous (Campanian) carbon isotope events, sea-level change and correlations of the Tethyan and Boreal realms. *Palaeogeography, Palaeoclimatology, Palaeoecology* **188**, 215–248.

- Jenkyns, H.C., Gale, A.S. & Cornfield, R.M., 1994: Carbon and oxygen isotope stratigraphy of the English chalk and Italian scaglia and its palaeoclimatic significance. *Geological Magazine* **131**, 1–34.
- Jørgensen, N.O., 1987: Oxygen and carbon isotope compositions of Upper Cretaceous chalk from the Danish sub-basin and the North Sea Central Graben. *Sedimentology* **34**, 559–570.
- Jørgensen, N.O., 1990: Geochemistry and chemostratigraphy of Upper Cretaceous and Lower Paleocene (Danian) chalk from Denmark. EFP-project No. 1313/86-4 and 1313/87-4. Geologisk Centralinstitut, Københavns Universitet.
- Kristensen, L., Dons, T., Maver, K.G. & Schiøler, P., 1995: A multidisciplinary approach to reservoir subdivision of the Maastrichtian chalk in the Dan Field, Danish North Sea. *AAPG Bulletin* **79**, 1650–1660.
- Lassen, S. & Rasmussen, J.A. 2004: High-resolution foraminiferal biostratigraphy of the Upper Maastrichtian – basal Danian strata, Danish Central Graben. A contribution to EFP-2001 (1313/01-0001). Danmarks og Grønlands Geologiske Undersøgelse Rapport **2004/87**.
- Li, L. & Keller, G., 1999: Variability in Late Cretaceous climate and deep waters: evidence from stable isotopes. *Marine Geology* **161**, 171–190.
- Lieberkind, K., Bang, I., Mikkelsen, N. & Nygaard, E., 1982: Late Cretaceous and Danian limestone. In Michelsen, O., (Eds): *Geology of the Danish Central Graben*. Geological Survey of Denmark Series **B 8**, 49-62.
- McCrea, J.M., 1950: The isotope chemistry of carbonates and a paleotemperature scale. *Journal of Chemical Physics* **18**, 849–857.
- Schiøler, P. 2004: Palynology of the Upper Maastrichtian, Danish Central Graben. A contribution to EFP-2001 (1313/01-0001). Danmarks og Grønlands Geologiske Undersøgelse Rapport **2004/84**.
- Schiøler, P. & Wilson, G.J., 1993: Maastrichtian dinoflagellate zonation in the Dan Field, Danish North Sea. *Review of Palaeobotany and Palynology* **78**, 321–351.
- Scholle, P.A. & Arthur, M.A., 1980: Carbon isotopes in Cretaceous pelagic limestones: potential stratigraphic and petroleum exploration tool. *AAPG Bulletin* **64**, 67–87.
- Scholle, P.A., 1977: Chalk diagenesis and its relation to petroleum exploration: oil from chalk, a modern miracle? *AAPG Bulletin* **61**, 982–1009.
- Scholle, P.A., Albrechtsen, T. & Tirsgaard, H., 1998: Formation and diagenesis of bedding cycles in uppermost Cretaceous chalks of the Dan Field, Danish North Sea. *Sedimentology* **45**, 223–243.
- Schönfeld, J., Sirocko, F. & Jørgensen, N.O., 1991: Oxygen isotope composition of Upper Cretaceous chalk at Lägerdorf (NW Germany): its original environmental signal and palaeotemperature interpretation. *Cretaceous Research* **12**, 27–46.
- Sheldon, E., 2004: High-resolution nannofossil biostratigraphy of the Upper Maastrichtian – Lower Danian chalk, Danish Central Graben. A contribution to EFP-2001 (1313/01-0001). Danmarks og Grønlands Geologiske Undersøgelse Rapport **2004/85**.
- Stage, M., 2001: Recognition of cyclicity in the petrophysical properties of a Maastrichtian pelagic chalk oil field reservoir from the Danish North Sea. *AAPG Bulletin* **85**, 2003–2015.



- Stüben, D., Kramar, U., Berner, Z.A., Meudt, M., Keller, G., Abramovich, D., Adatte, T., Hambach, U. & Stinnesbeck, W., 2003: Late Maastrichtian paleoclimatic and paleoceanographic changes inferred from Sr/Ca ratio and stable isotopes. *Palaeogeography, Palaeoclimatology, Palaeoecology* **199**, 107–127.
- Surlyk, F., 1984: The Maastrichtian stage in NW Europe, and its brachiopod zonation. *Bulletin of the Geological Society of Denmark* **33**, 217–223.
- Toft, J., Albrechtsen, T. & Tirsgaard, H., 1996: Use of cyclostratigraphy in Danish chalks for field development and appraisal. Fifth North Sea Chalk Symposium. October 7–9, 1996, Reims, France.

# Table 1

Carbon and oxygen isotope analysis for the E-5X and M-10X wells. Data are listed by wells and sorted by depth. All depths refer to core depth. Lithologic types: B, bioturbated; (L), weakly laminated; L, laminated.

Sample ID	Well	Depth m	Core depth		Lab ID	$\delta^{13}\text{C}$ ‰ V-PDB	$\delta^{18}\text{O}$ ‰ V-PDB	Litho type	Stratigraphy Units	Comments
			feet	inch						
E-5-51	E-5X	2075.43	6809	2	14963	0.88	-3.13	B	Danian	
E-5-50	E-5X	2076.17	6811	7	14962	1.08	-3.43	B	Danian	
E-5-49	E-5X	2076.96	6814	2	14961	1.09	-2.87	B	Danian	
E-5-48	E-5X	2078.02	6817	8	14960	1.44	-2.51	B	Danian	
E-5-47	E-5X	2078.33	6818	8	14959	1.71	-2.53	B	Danian	
E-5-46	E-5X	2078.61	6819	7	14958	1.71	-2.47	B	Maastrichtian	?Danian chalk
E-5-45	E-5X	2078.99	6820	10	14957	1.49	-3.64	B	A	
E-5-44	E-5X	2079.75	6823	4	14955	1.58	-3.94	B	A	
E-5-43	E-5X	2081.17	6828	0	14954	1.63	-3.96	B	A	
E-5-42	E-5X	2081.71	6829	9	14953	1.70	-3.28	B	B	
E-5-41	E-5X	2082.44	6832	2	14965	1.69	-3.39	B	B	
E-5-40	E-5X	2083.51	6835	8	14951	1.65	-4.00	B	B	
E-5-39	E-5X	2085.42	6841	11	14950	1.74	-3.43	B	B	
E-5-38	E-5X	2086.00	6843	10	14949	1.73	-3.83	B	B	
E-5-37	E-5X	2086.91	6846	10	14948	1.77	-3.67	B	B	
E-5-36	E-5X	2087.83	6849	10	14964	1.71	-3.60	(L)	B	
E-5-35	E-5X	2091.54	6862	0	14945	1.76	-2.93	B	C	
E-5-34	E-5X	2092.35	6864	8	14944	1.78	-3.05	B	C	
E-5-33	E-5X	2093.29	6867	9	14943	1.71	-3.20	B	C	
E-5-32	E-5X	2094.15	6870	7	14942	1.73	-3.15	B	C	
E-5-31	E-5X	2095.60	6875	4	14941	1.68	-3.60	B	C	
E-5-30	E-5X	2096.29	6877	7	14940	1.67	-3.30	B	C	
E-5-29	E-5X	2097.10	6880	3	14939	1.63	-3.61	B	C	
E-5-28	E-5X	2098.68	6885	5	14938	1.61	-3.26	B	C	
E-5-27	E-5X	2098.95	6886	4	14937	1.55	-3.29	B	D	
E-5-26	E-5X	2100.66	6891	11	14935	1.62	-3.39	B	D	
E-5-25	E-5X	2101.24	6893	10	14934	1.60	-3.82	B	D	
E-5-24	E-5X	2102.05	6896	6	14933	1.62	-4.11	(L)	D	
E-5-23	E-5X	2103.30	6900	7	14932	1.68	-3.68	B	D	
E-5-22	E-5X	2103.78	6902	2	14931	1.63	-3.54	B	D	
E-5-21	E-5X	2105.20	6906	10	14930	1.68	-3.83	B	D	
E-5-20	E-5X	2106.14	6909	11	14929	1.77	-3.55	B	D	
E-5-19	E-5X	2106.55	6911	3	14928	1.74	-3.68	B	D	
E-5-18	E-5X	2107.54	6914	6	14927	1.74	-3.72	(L)	D	
E-5-17	E-5X	2108.86	6918	10	14925	1.76	-4.03	B	D	
E-5-16	E-5X	2110.49	6924	2	14924	1.82	-4.03	B	D	
E-5-15	E-5X	2110.89	6925	6	14923	1.76	-3.70	B	D	

Table 1 continued.

Sample ID	Well	Depth m	Core depth feet    inch	Lab ID	$\delta^{13}\text{C}$ ‰ V- PDB	$\delta^{18}\text{O}$ ‰ V- PDB	Litho type	Stratigraphy Units	Comments
E-5-14	E-5X	2112.42	6930    6	14922	1.79	-3.67	B	D	
E-5-13	E-5X	2114.02	6935    9	14921	1.88	-3.45	B	E	
E-5-12	E-5X	2114.96	6938    10	14920	1.82	-3.68	B	E	
E-5-11	E-5X	2115.49	6940    7	14919	1.90	-3.36	B	E	
E-5-10	E-5X	2116.63	6944    4	14918	1.79	-3.40	B	E	
E-5-9	E-5X	2117.06	6945    9	14915	1.79	-3.37	B	E	
E-5-8	E-5X	2118.79	6951    5	14917	1.85	-3.80	B	E	
E-5-7	E-5X	2119.93	6955    2	14913	1.83	-3.62	B	E	
E-5-6	E-5X	2121.46	6960    2	14912	1.83	-3.39	B	E	
E-5-5	E-5X	2121.76	6961    2	14911	1.86	-3.43	B	E	
E-5-4	E-5X	2122.93	6965    0	14858	1.88	-3.81	B	E	
E-5-3	E-5X	2124.02	6968    7	14857	1.88	-3.68	B	E	
E-5-2	E-5X	2124.96	6971    8	14856	1.88	-3.46	B	E	
E-5-1	E-5X	2125.98	6975    0	14855	no data	no data	B	E	
I-76	M-10X	1960.96	6433    7	14703	0.74	-5.01	B	Danian	
I-75	M-10X	1961.26	6434    7	14701	1.03	-3.39	B	Danian	
I-74	M-10X	1961.95	6436    10	14700	1.50	-3.18	B	Danian	
I-73	M-10X	1962.56	6438    10	14699	1.51	-3.50	B	Danian	
I-72	M-10X	1962.73	6439    5	14698	1.55	-2.32	B	Maastrich- tian	?Danian chalk
I-71	M-10X	1963.09	6440    7	14697	1.29	-4.02	B	A	
I-70	M-10X	1963.50	6441    11	14696	1.21	-4.08	B	A	
I-69	M-10X	1963.95	6443    5	14695	1.43	-4.08	B	A	
I-68	M-10X	1964.39	6444    10	14694	1.35	-4.51	B	A	
I-67	M-10X	1965.40	6448    2	14693	1.52	-4.37	B	A	
I-66	M-10X	1966.34	6451    3	14691	1.45	-4.56	B	A	
I-65	M-10X	1967.20	6454    1	14690	1.52	-4.38	B	A	
I-64	M-10X	1968.02	6456    9	14689	1.58	-4.01	B	A	
I-63	M-10X	1969.01	6460    0	14688	1.38	-4.64	B	B	
I-62	M-10X	1969.92	6463    0	14687	1.47	-4.75	B	B	
I-61	M-10X	1971.50	6468    2	14686	1.47	-4.89	B	B	
I-60	M-10X	1972.36	6471    0	14685	1.48	-4.92	B	B	
I-59	M-10X	1973.20	6473    9	14707	1.49	-4.79	B	B	
I-58	M-10X	1974.19	6477    0	14683	1.49	-4.30	B	B	Sub sample 2
I-58	M-10X	1974.19	6477    0	14731	1.44	-4.31	B	B	Sub sample 1
I-57	M-10X	1975.41	6481    0	14682	1.47	-4.46	B	B	
I-56	M-10X	1976.27	6483    10	14680	1.57	-4.19	B	C	
I-55	M-10X	1977.54	6488    0	14679	1.51	-4.71	B	C	
I-54	M-10X	1978.08	6489    9	14678	1.56	-4.81	B	C	
I-53	M-10X	1979.80	6495    5	14677	1.55	-4.29	B	C	
I-52	M-10X	1980.39	6497    4	14676	1.52	-4.99	B	C	
I-51	M-10X	1980.87	6498    11	14675	1.56	-3.42	B	C	
I-50	M-10X	1981.23	6500    1	14674	1.48	-5.08	B	C	

Table 1 continued.

Sample ID	Well	Depth m	Core depth feet inch	Lab ID	$\delta^{13}\text{C}$ ‰ V-PDB	$\delta^{18}\text{O}$ ‰ V-PDB	Litho type	Stratigraphy Units	Comments
I-49	M-10X	1981.76	6501 10	14673	1.54	-4.30	B	C	
I-48	M-10X	1982.60	6504 7	14672	1.49	-4.54	B	C	
I-47	M-10X	1983.56	6507 9	14670	1.48	-4.88	B	C	
I-46	M-10X	1984.43	6510 7	14669	1.41	-4.91	B	C	
I-45	M-10X	1985.29	6513 5	14668	1.45	-4.75	B	C	
I-44	M-10X	1985.95	6515 7	14667	1.48	-3.97	B	C	
I-43	M-10X	1988.36	6523 6	14666	1.45	-4.21	B	C	Sub sample 1
I-43	M-10X	1988.36	6523 6	14734	1.45	-4.18	B	C	Duplicate sample 1
I-43	M-10X	1988.36	6523 6	14753	1.49	-4.08	B	C	Sub sample 2
I-42	M-10X	1989.10	6525 11	14665	1.30	-4.54	B	D	sub sample 1
I-42	M-10X	1989.10	6525 11	14733	1.30	-4.52	B	D	Duplicate sample 1
I-42	M-10X	1989.10	6525 11	14752	1.27	-4.57	B	D	Sub sample 2
I-41	M-10X	1990.01	6528 11	14664	1.50	-4.23	B	D	Sub sample 1
I-41	M-10X	1990.01	6528 11	14750	1.48	-4.15	B	D	Duplicate sample 1
I-41	M-10X	1990.01	6528 11	14751	1.47	-4.30	B	D	Sub sample 2
I-40	M-10X	1990.55	6530 8	14663	1.49	-5.04	(L)	D	
I-39	M-10X	1991.26	6533 0	14662	1.56	-4.49	B	D	
I-38	M-10X	1993.04	6538 10	14661	1.59	-4.44	L	D	
I-37	M-10X	1994.18	6542 7	14659	1.62	-4.82	(L)	D	
I-36	M-10X	1995.35	6546 5	14658	1.62	-4.54	B	D	
I-35	M-10X	1996.08	6548 10	14657	1.64	-4.54	B	D	
I-34	M-10X	1997.10	6552 2	14656	1.66	-4.42	B	D	
I-33	M-10X	1997.61	6553 10	14655	1.66	-4.54	L	D	
I-32	M-10X	1999.06	6558 7	14654	1.76	-4.17	B	E	
I-31	M-10X	2000.07	6561 11	14653	1.74	-4.68	(L)	E	
I-30	M-10X	2000.43	6563 1	14652	1.67	-4.60	L	E	
I-29	M-10X	2001.52	6566 8	14651	1.75	-4.42	B	E	
I-28	M-10X	2002.82	6570 11	14706	1.67	-4.47	B	E	
I-27	M-10X	2004.11	6575 2	14648	1.69	-4.53	B	E	
I-26	M-10X	2004.70	6577 1	14705	1.67	-4.84	B	E	
I-25	M-10X	2005.20	6578 9	14646	1.71	-4.59	B	E	
I-24	M-10X	2006.35	6582 6	14645	1.75	-4.05	B	E	
I-23	M-10X	2007.49	6586 3	14644	1.74	-4.91	(L)	E	
I-22	M-10X	2008.66	6590 1	14643	1.83	-3.97	B	E	
I-21	M-10X	2009.14	6591 8	14642	1.79	-4.33	L	E	
I-20	M-10X	2011.20	6598 5	14641	1.74	-4.70	B	E	
I-19	M-10X	2011.93	6600 10	14640	1.75	-4.28	B	E	
I-18	M-10X	2013.20	6605 0	14638	1.84	-4.20	(L)	E	
I-17	M-10X	2014.12	6608 0	14637	1.86	-4.10	(L)	E	
I-16	M-10X	2014.91	6610 7	14636	1.77	-4.40	B	E	
DS-I-21	M-10X	2015.21	6611 7	14831	1.74	-4.15	B	F	

Table 1 continued.

Sample	Well	Depth	Core depth		Lab ID	$\delta^{13}\text{C}$	$\delta^{18}\text{O}$	Litho	Stratigraphy	Comments
ID		m	feet	inch		‰ V-PDB	‰ V-PDB	type	Units	
DS-I-20	M-10X	2015.44	6612	4	14830	1.73	-4.42	B	F	
DS-I-19	M-10X	2015.54	6612	8	14829	1.68	-4.59	(L)	F	
DS-I-18	M-10X	2015.67	6613	1	14828	1.76	-4.31	B	F	
DS-I-17	M-10X	2015.79	6613	6	14826	1.75	-4.52	B	F	
I-15	M-10X	2015.97	6614	1	14635	1.76	-4.65	B	F	
DS-I-15	M-10X	2016.07	6614	5	14825	1.72	-4.51	B	F	
DS-I-14	M-10X	2016.18	6614	9	14824	1.69	-4.67	L	F	
DS-I-13	M-10X	2016.25	6615	0	14823	1.69	-4.30	L	F	
DS-I-12	M-10X	2016.35	6615	4	14822	1.67	-4.66	L	F	
DS-I-11	M-10X	2016.43	6615	7	14821	1.77	-4.57	B	F	
DS-I-10	M-10X	2016.53	6615	11	14820	1.79	-4.17	B	F	
DS-I-9	M-10X	2016.63	6616	3	14819	1.72	-4.80	B	F	
I-14	M-10X	2016.84	6616	11	14634	1.79	-4.55	B	F	Sub sample 1
I-14	M-10X	2016.84	6616	11	14704	1.78	-4.56	B	F	Duplicate sample 1
DS-I-7	M-10X	2016.91	6617	2	14818	1.78	-4.45	(L)	F	
DS-I-6	M-10X	2017.04	6617	7	14758	1.76	-4.71	(L)	F	
DS-I-5	M-10X	2017.17	6618	0	14757	1.79	-4.47	L	F	
DS-I-4	M-10X	2017.29	6618	5	14756	1.77	-4.64	L	F	
DS-I-3	M-10X	2017.34	6618	7	14755	1.70	-4.54	B	F	
I-13	M-10X	2017.47	6619	0	14633	1.81	-3.82	B	F	
DS-I-1	M-10X	2017.60	6619	5	14754	1.80	-4.31	B	F	
I-12	M-10X	2018.54	6622	6	14632	1.83	-4.02	B	F	
I-11	M-10X	2019.73	6626	5	14631	1.74	-4.63	(L)	F	
I-10	M-10X	2020.57	6629	2	14630	1.79	-4.26	(L)	F	
I-9	M-10X	2021.31	6631	7	14628	1.90	-4.23	B	F	
I-8	M-10X	2022.35	6634	12	14627	1.88	-4.44	L	F	
I-7	M-10X	2023.06	6637	4	14626	1.91	-4.44	L	F	
I-6	M-10X	2024.13	6640	10	14625	no data	no data	B	F	
I-5	M-10X	2025.12	6644	1	14624	1.96	-4.16	B	F	
I-4	M-10X	2026.01	6647	0	14623	1.82	-4.95	(L)	G	
I-3	M-10X	2026.97	6650	2	14622	1.87	-4.63	L	G	
I-2	M-10X	2027.71	6652	7	14621	1.87	-4.39	B	G	
I-1	M-10X	2028.62	6655	7	14620	1.92	-4.67	B	G	

Table 1 continued (data on working standards).

Sample ID	Well	Depth m	Core depth		Lab ID	$\delta^{13}\text{C}$	$\delta^{18}\text{O}$	Litho type	Stratigraphy Units	Comments
			feet	inch		‰ V-PDB	‰ V-PDB			
LEO working Standard					L14854	1.97	-1.92			
LEO working Standard					L14859	1.96	-1.88			
LEO working Standard					L14860	1.95	-1.99			
LEO working Standard					L14926	1.95	-1.93			
LEO working Standard					L14936	1.95	-1.95			
LEO working Standard					L14956	1.98	-1.93			
LEO working Standard					L14966	1.96	-1.91			
LEO working Standard					L14718	1.98	-1.89			
LEO working Standard					L14728	1.95	-1.93			
LEO working Standard					L14735	1.94	-1.95			
LEO working Standard					L14759	1.94	-1.95			
LEO working Standard					L14827	1.97	-1.91			
LEO working Standard					L14837	1.97	-1.95			
LEO working Standard					L14853	1.97	-1.93			
					average of working standards	1.96	-1.93			
					standard deviation on mean	0.01	0.03			

## Table 2

Summary of stratigraphic data in the M-10X and E-5X wells. The reported levels correspond to top level. All depths refer to core depth. Note that the positions of the UC20b/c and FCS23a/b boundaries in the wells are uncertain. Data have been included from Ineson (2004), Schiøler (2004), Sheldon (2004) and Lassen & Rasmussen (2004).

Stage	Type	Zone	E-5X		Thick ness M	M-10X		Thickness m
			Feet	m		feet	m	
K/T Hardground	Lithostratigraphic		6819.3	2078.5		6439.1	1962.6	
Danian	Nannofossil Zone	NNTP2g	?			?		
Danian	Nannofossil Zone	NNTP2f	6809.0	2075.4	1.5	?		
Danian	Nannofossil Zone	NNTP2e	6814.0	2076.9	1.6	?		
Upper Maastr.	Nannofossil Zone	UC20d	6819.3	2078.5	17.1	6439.1	1962.6	20.9
Upper Maastr.	Nannofossil Zone	UC20c	6875.3	2095.6	10.6	6507.7	1983.5	7.8
Upper Maastr.	Nannofossil Zone	UC20b	6910.3	2106.2		6533.2	1991.3	31.7
Upper Maastr.	Nannofossil Zone	UC20a	Np			6637.3	2023.1	
Upper Maastr.	Dinoflagellate Zone	Pgr	6819.3	2078.5	16.3	6439.1	1962.6	19.8
Upper Maastr.	Dinoflagellate Zone	Hbo	6872.7	2094.8	16.3	6504.0	1982.4	14.7
Upper Maastr.	Dinoflagellate Zone	Pde	6926.2	2111.1		6552.3	1997.1	23.7
Upper Maastr.	Dinoflagellate Zone	Ico	Np			6629.9	2020.8	
Upper Maastr.	Foraminifer Zone	FCS23b	6819.3	2078.5	18.9	6439.1	1962.6	26.3
Upper Maastr.	Foraminifer Zone	FCS23a	6881.4	2097.5		6525.3	1988.9	

?: not identified

Np: not present

### Table 3

Summary of chemostratigraphic units in the M-10X and E-5X wells. The reported levels correspond to top level. All depths refer to core depth.

Stage	Unit	E-5X		M-10X		Thickness	
		Feet	M	feet	m	m	m
Danian -Upper Maastrichtian		6819.6*	2078.6	6439.4*	1962.7		
Upper Maastrichtian	A	6820.8	2079.0	2.7	6440.6	1963.1	5.9
Upper Maastrichtian	B	6829.8	2081.7	7.8	6460.0	1969.0	7.3
Upper Maastrichtian	C**	6855.5	2089.6	9.4	6483.8	1976.3	12.8
Upper Maastrichtian	D	6886.3	2099.0	15.1	6525.9***	1989.1***	10.0
Upper Maastrichtian	E	6935.8	2114.0		6558.6	1999.1	16.2
Upper Maastrichtian	F	Np			6611.6	2015.2	10.8
Upper Maastrichtian	G	Np			6647.0	2026.0	

Np: not present

\* Base level.

\*\*Gap between 6850-6861 feet in the E-5X well. Unit C/B boundary is placed arbitrarily.

\*\*\* Alternatively, the top level might be positioned at 1984m, 6510 feet (see text for discussion).



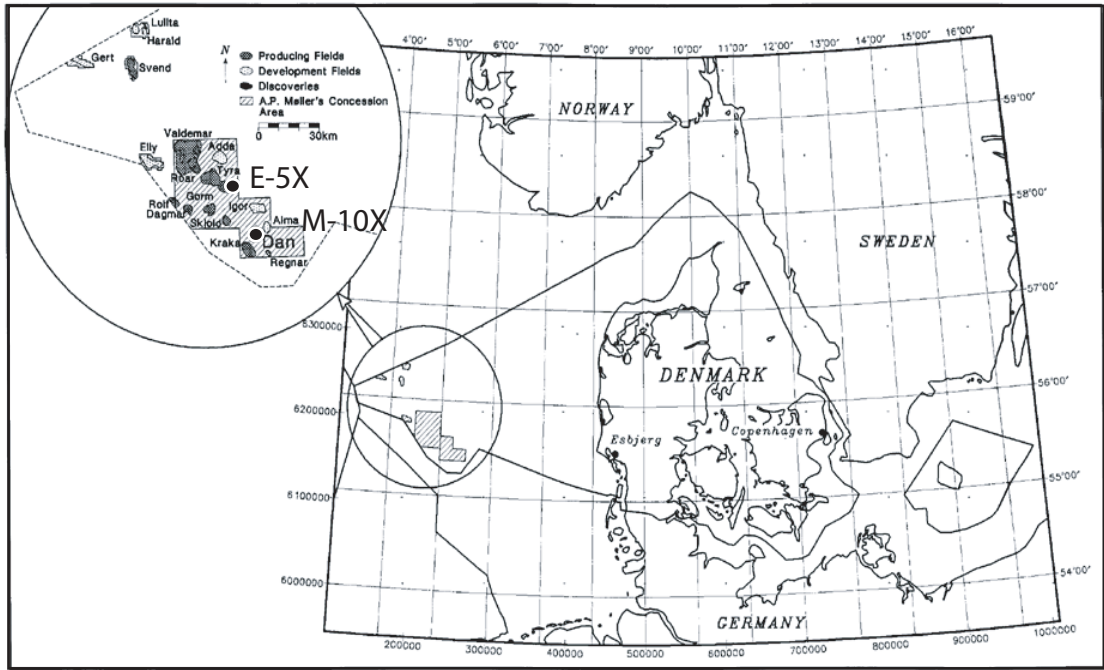


Figure 1: Location of the M-10X and E-5X wells (modified from Scholle *et al.* 1998).

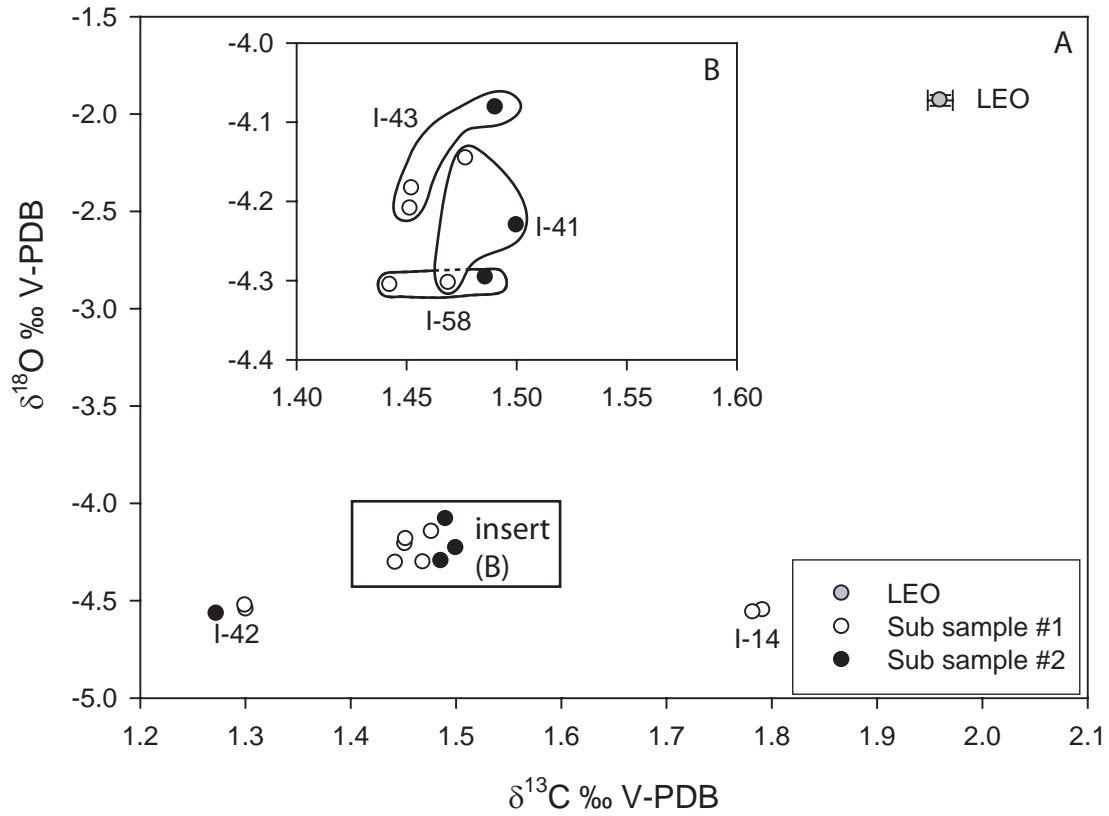


Figure 2: Comparison between  $\delta^{13}\text{C}$  and  $\delta^{18}\text{O}$  variation of the LEO working standards (mean value of 14 samples) and samples measured in duplicate or where the samples have been sampled twice (subsample 1 and subsample 2). Error bars indicate standard deviation on mean. Data are presented in Table 1.

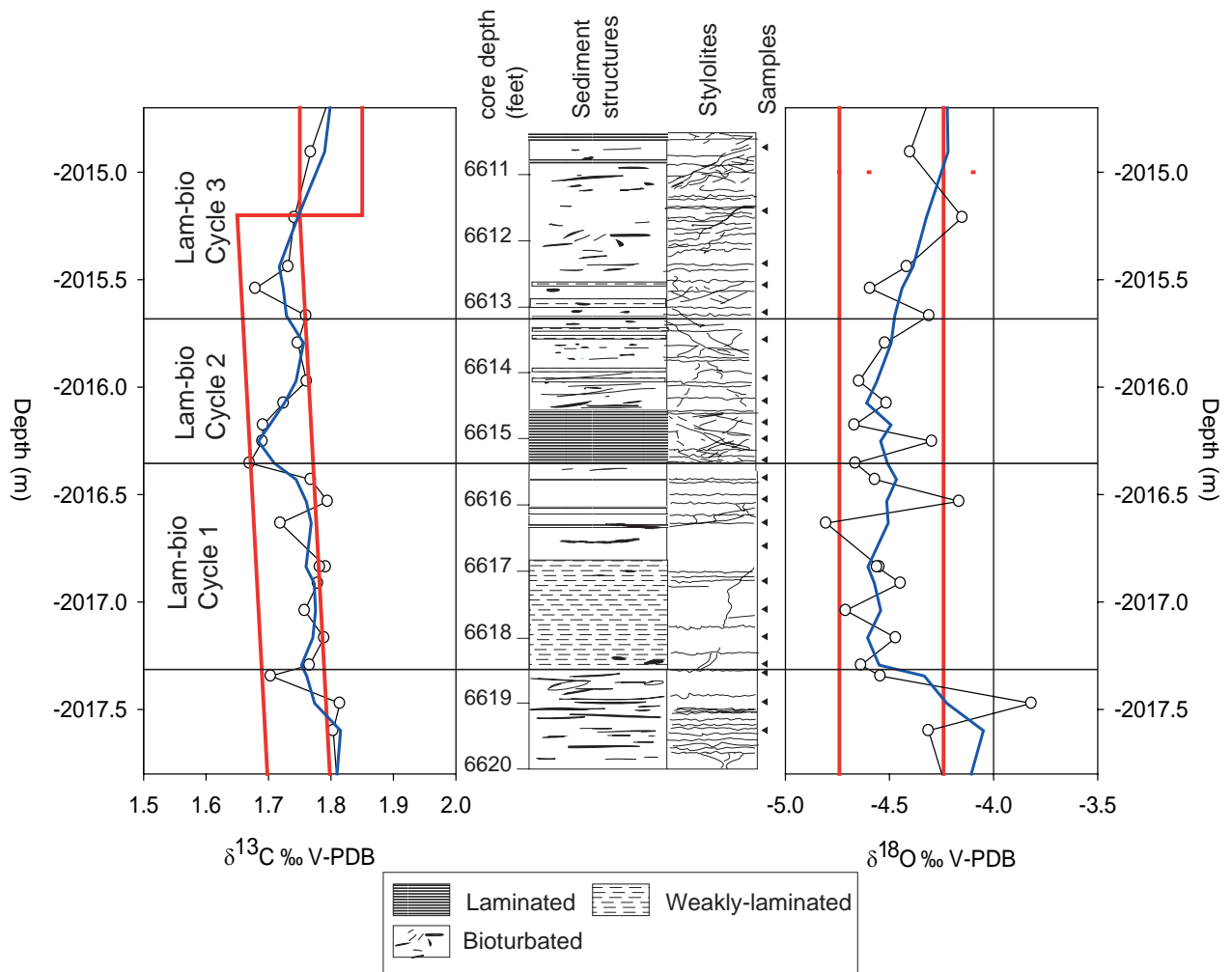


Figure 3: Detail of the stratigraphical variation in  $\delta^{13}\text{C}$ - and  $\delta^{18}\text{O}$ -isotopic values in the M-10X well together with a lithologic log including primary structures and secondary cross-cutting structure (stylolites and fractures). The data envelope of 0.1 ‰ for  $\delta^{13}\text{C}$  and 0.5 ‰ for  $\delta^{18}\text{O}$  represent the interpreted m-scale variation in the data material. A running average of 3 data points is included.

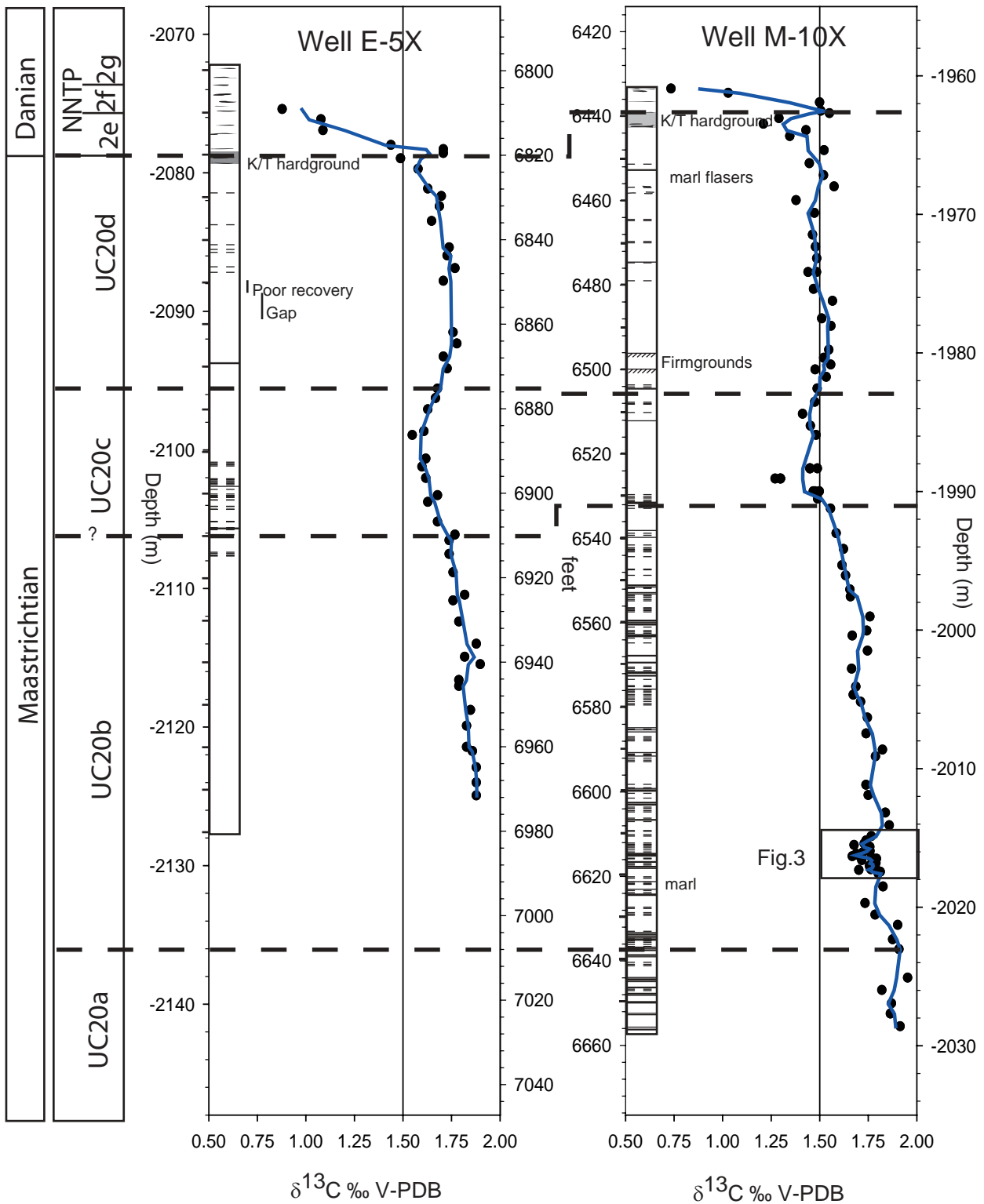


Figure 4: Stratigraphical variation of  $\delta^{13}\text{C}$  data in the M-10X and E-5X wells. A running average of three data points has been included. A reference line of 1.5 ‰ is shown. Simplified lithologic logs indicate location of K/T boundary hardground, flint nodules (black outline) and degree of lamination (weak lamination: broken line; laminated: unbroken line). Stratigraphical data are according to Table 2.

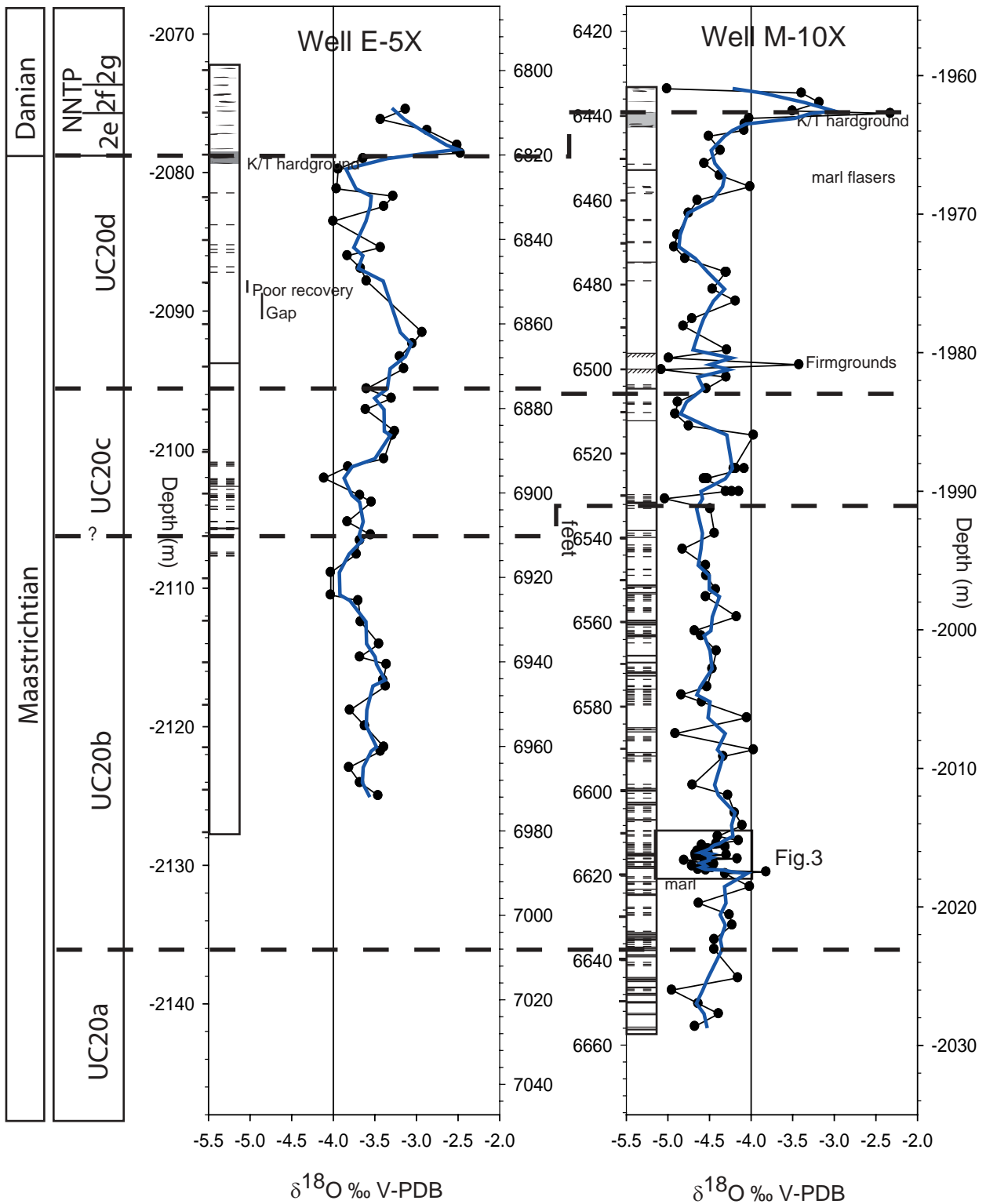


Figure 5: Stratigraphical variation of  $\delta^{18}\text{O}$  values in the M-10X and E-5X wells. A running average of three data points has been included. A reference line of  $-4.0$  ‰ is shown as graphic aid. Simplified lithologic logs indicate location of K/T boundary hardground, flint nodules (black outline), and degree of lamination (weak lamination: broken line; laminated: unbroken line). Stratigraphical data are according to Table 2.

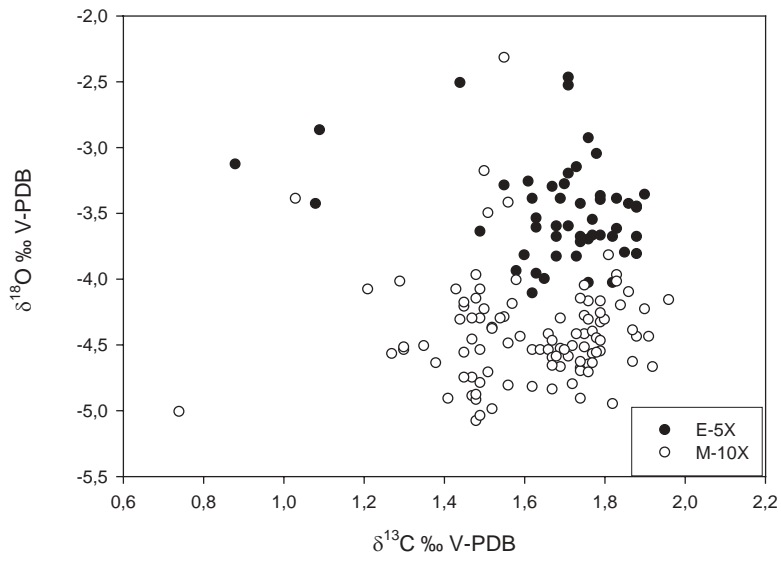


Figure 6:  $\delta^{13}\text{C}$  versus  $\delta^{18}\text{O}$  for all samples from the M-10X and E-5X wells.

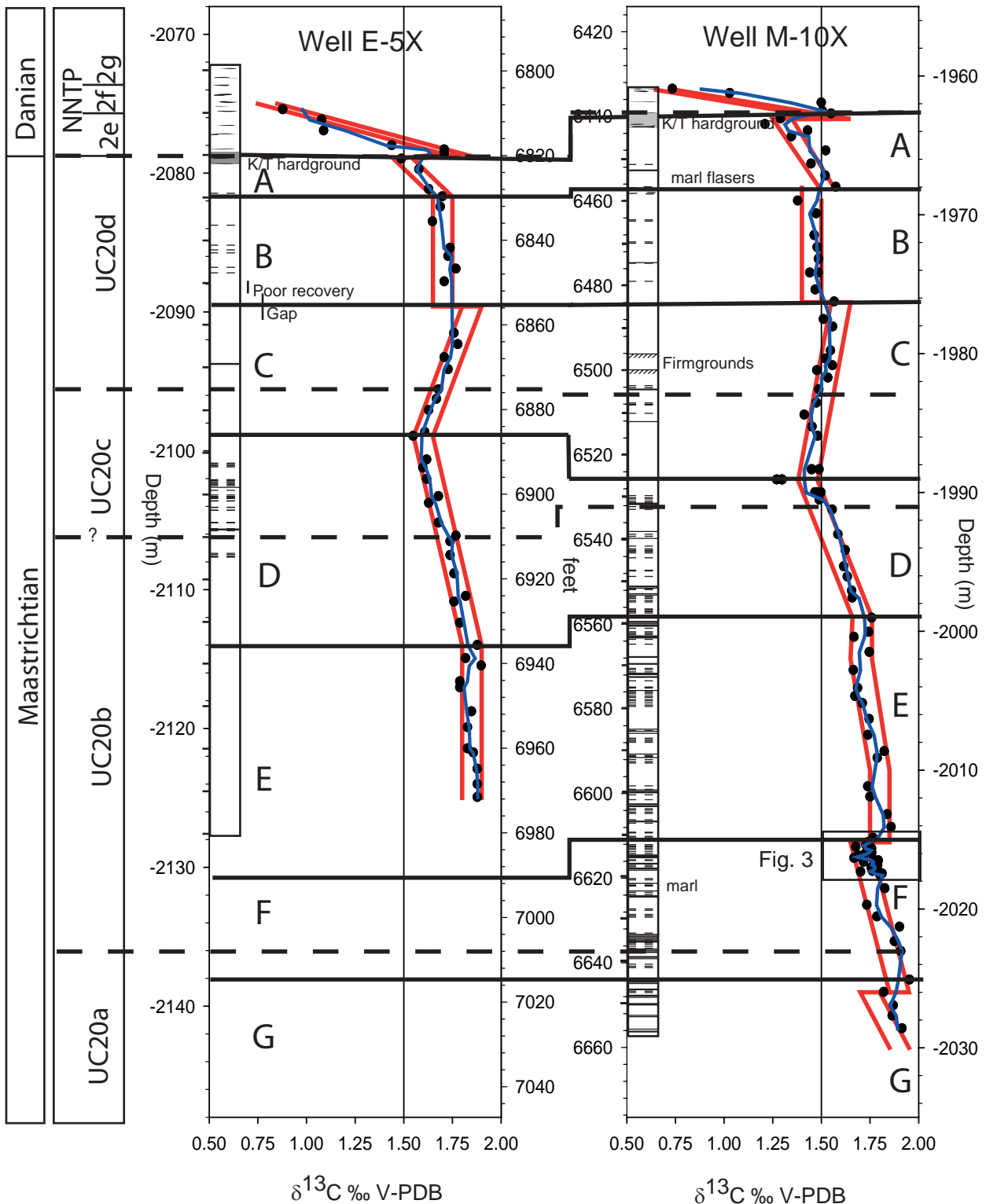


Figure 7: Chemostratigraphic correlation between the M-10X and E-5X wells based on the stratigraphical variation in  $\delta^{13}\text{C}$  values. Seven chemo stratigraphical units (Unit A though Unit G) have been constructed. See text for explanation. The data envelopes of 0.1 ‰ are inferred from Figure 3. A reference line of 1.5 ‰ is show. Simplified lithologic logs indicate location of K/T boundary hardground, flint nodules (black outline) and degree of lamination (weak lamination: broken line and laminated: unbroken line). Stratigraphical data are according to Table 2.

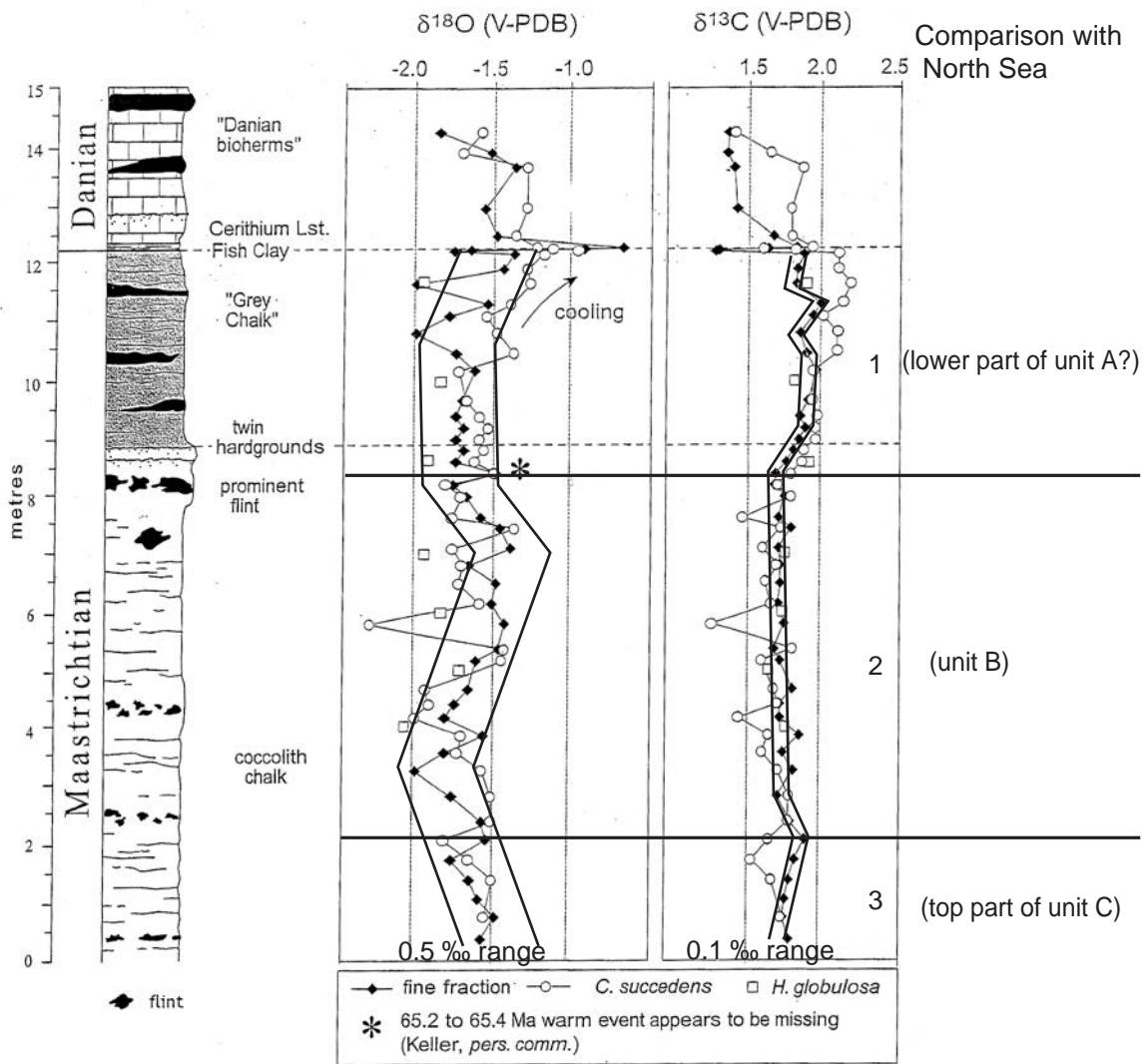


Figure 8. Example of an Upper Maastrichtian to lower Danian  $\delta^{18}\text{O}$  and  $\delta^{13}\text{C}$  isotope study at Stevns Klint, Denmark. Figure is from Hart *et al.* (2004). Data envelopes of 0.5 ‰ ( $\delta^{18}\text{O}$ ) and 0.1 ‰ ( $\delta^{13}\text{C}$ ) have been used to evaluate the stratigraphical variation. Based on the  $\delta^{13}\text{C}$  variation three chemostratigraphic units have been identified and correlated to the North Sea units.



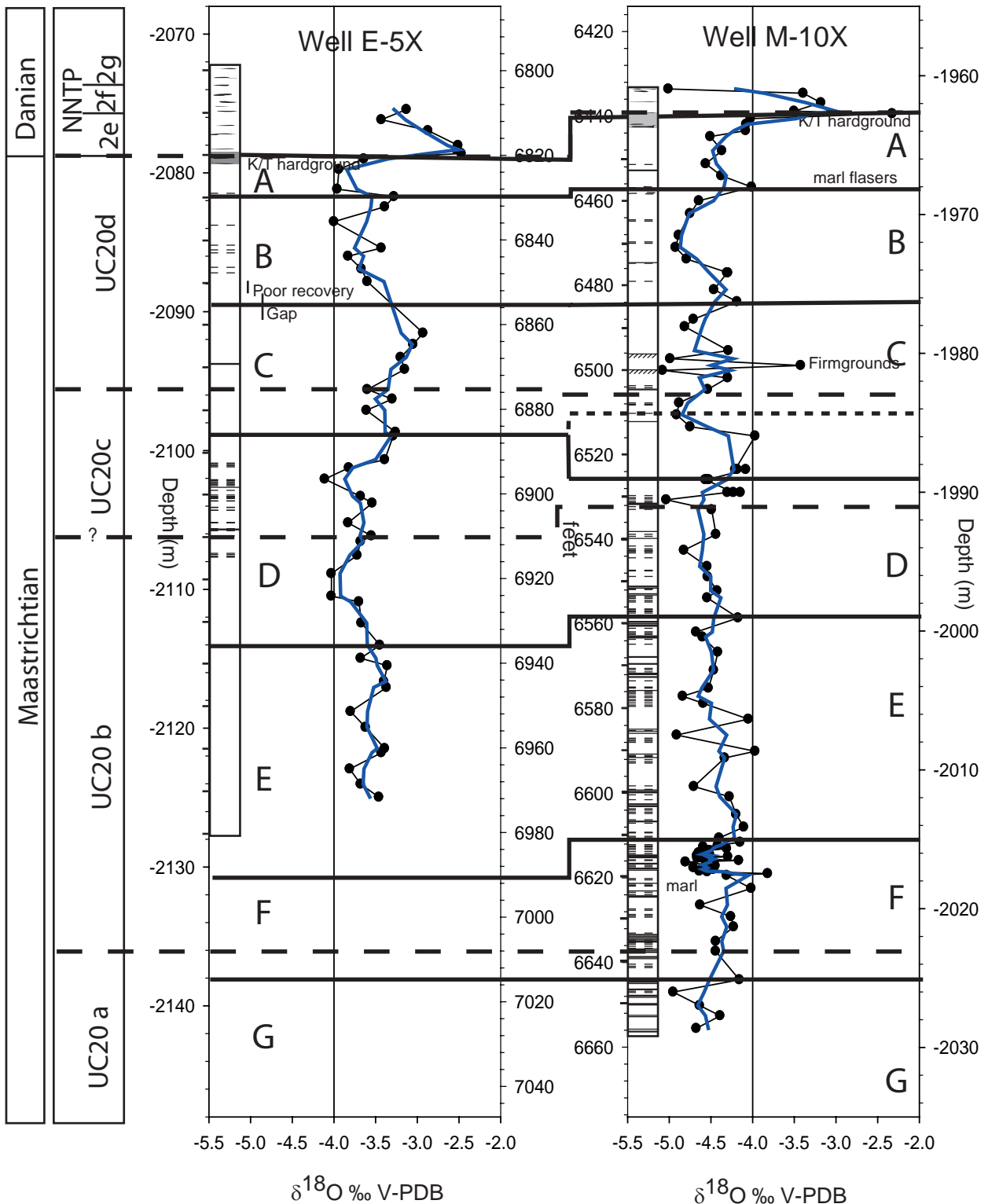


Figure 9. Stratigraphical variation of  $\delta^{18}\text{O}$  values in the M-10X and E-5X wells. Chemostratigraphic units are included from Figure 7. A running average of three data points has been included. A reference line of  $-4.0$  ‰ is shown as graphic aid. Simplified lithologic logs indicate location of K/T boundary hardground, flint nodules (black outline) and degree of lamination (weak lamination: broken line and laminated: unbroken line). Stratigraphical data are according to Table 2. An alternative position of the C/B unit boundary in M-10X well is indicated with broken line (see discussion in text).

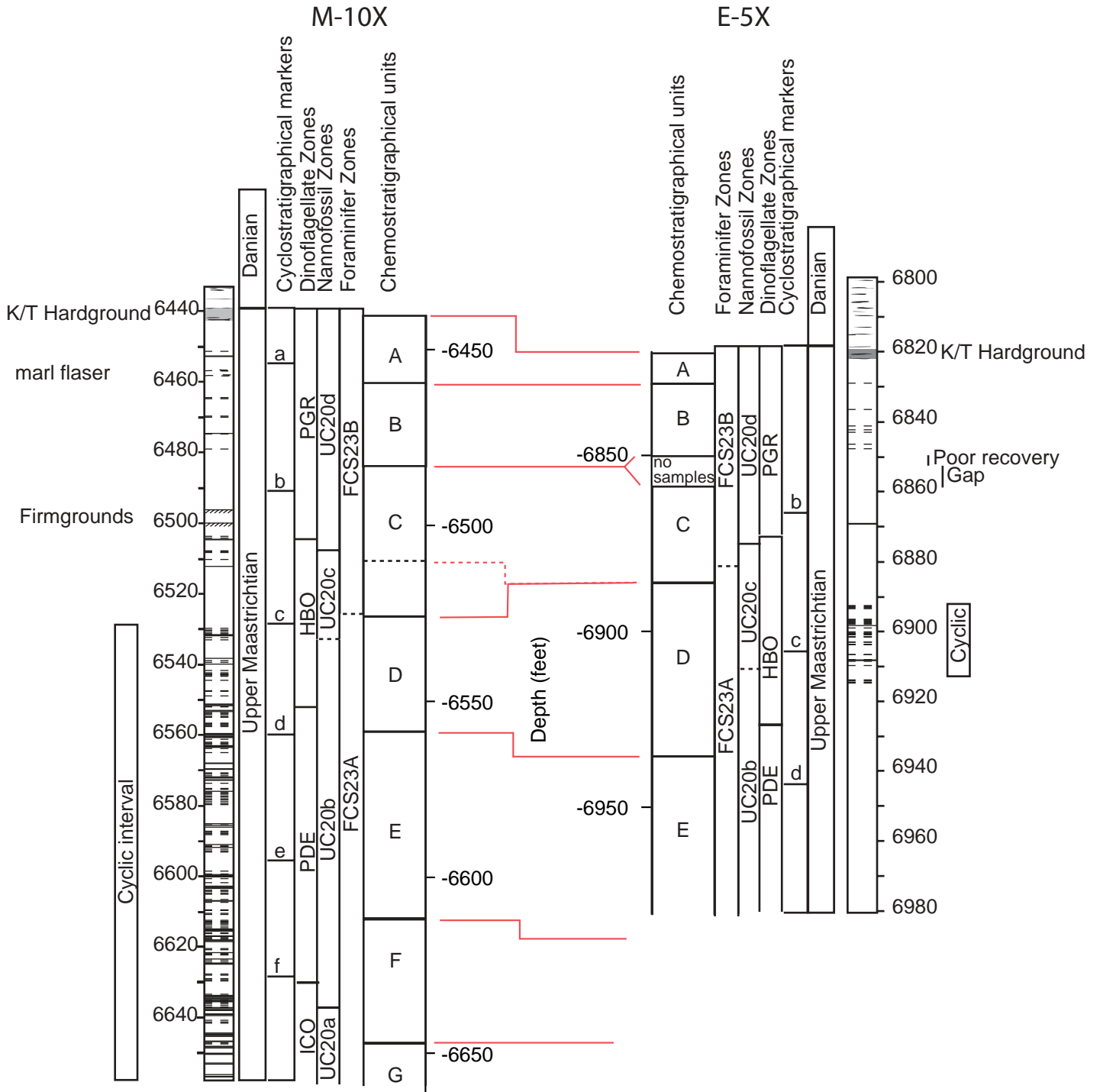


Figure 10: Comparison of chemostratigraphic, biostratigraphic, cyclostratigraphic (Toft *et al.* 1996; Damholt 2003) and lithologic information available for the M-10X and E-5X wells. Chemo- and biostratigraphic data are from Table 2 and 3.

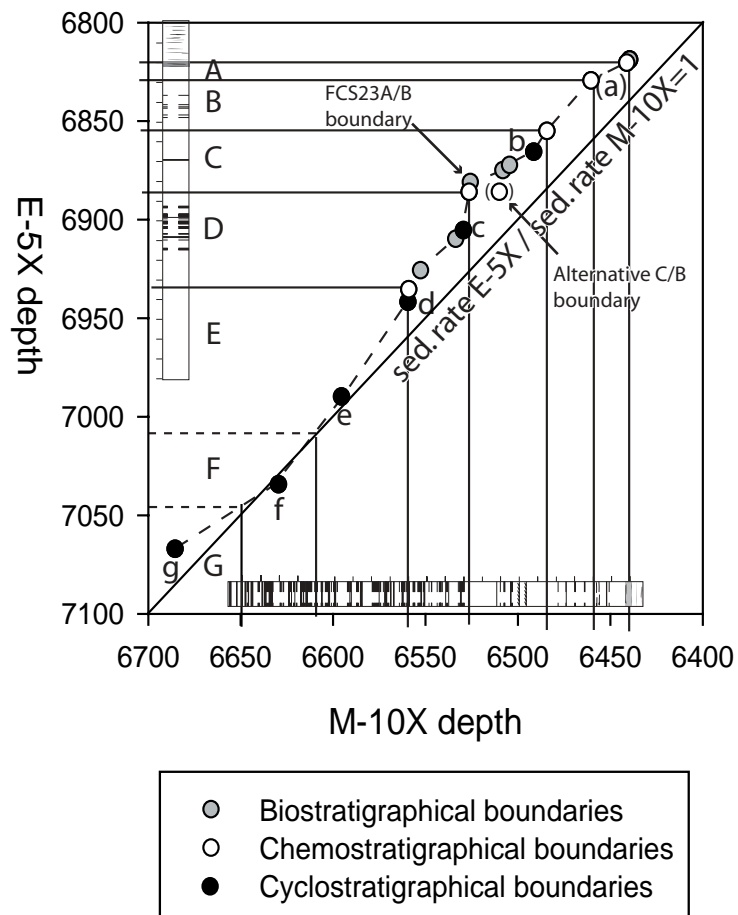


Figure 11: Thickness relationship between the M-10X and E-5X wells based on bio- chemo- and cyclostratigraphic correlation. Data are based on Figure 10. Capital letters refers to chemostratigraphic units; other letters refers to cyclostratigraphic markers as defined by Toft *et al.* (1996).

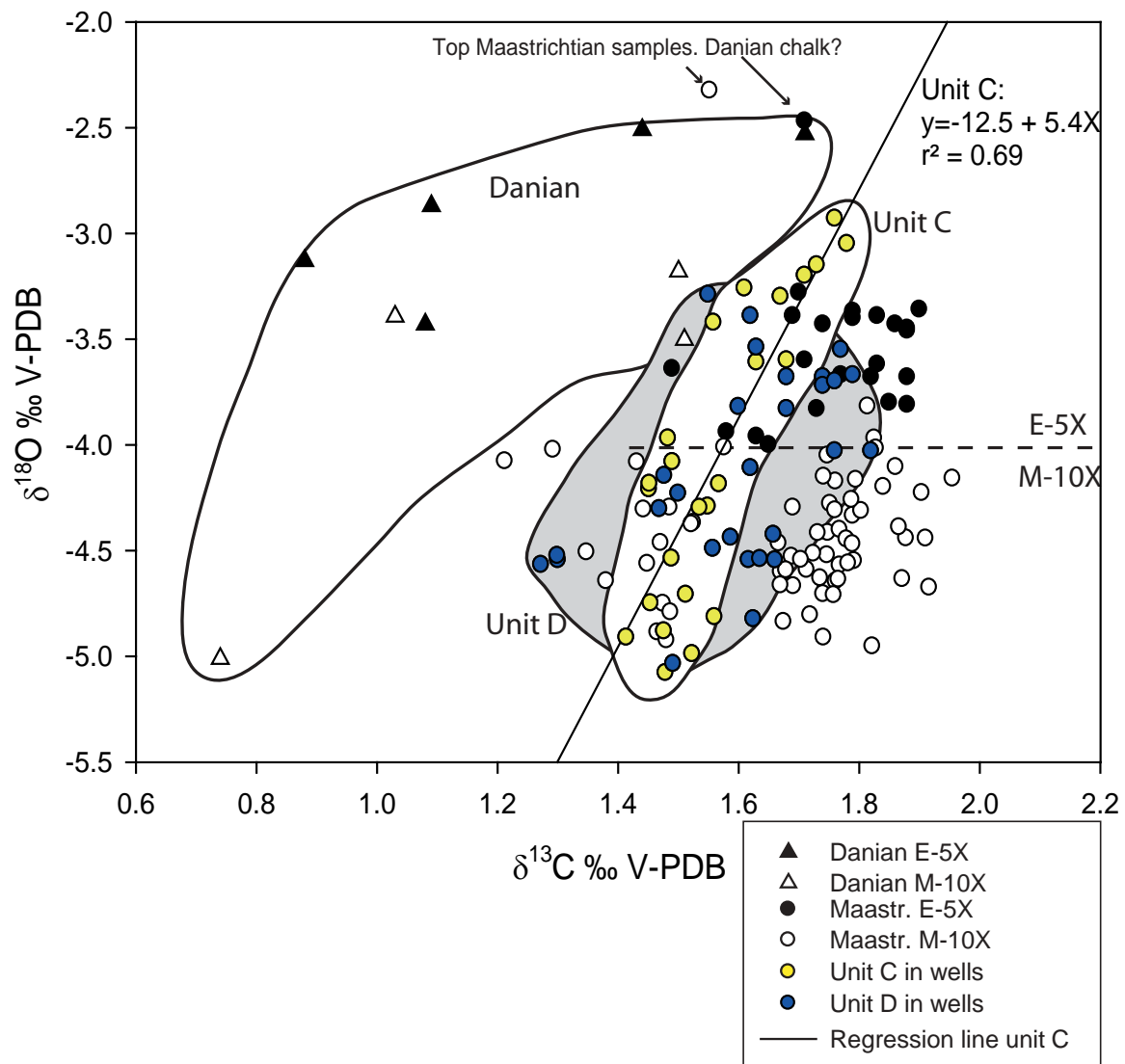


Figure 12: Variation in  $\delta^{13}\text{C}$  versus  $\delta^{18}\text{O}$  values according to stratigraphical units.

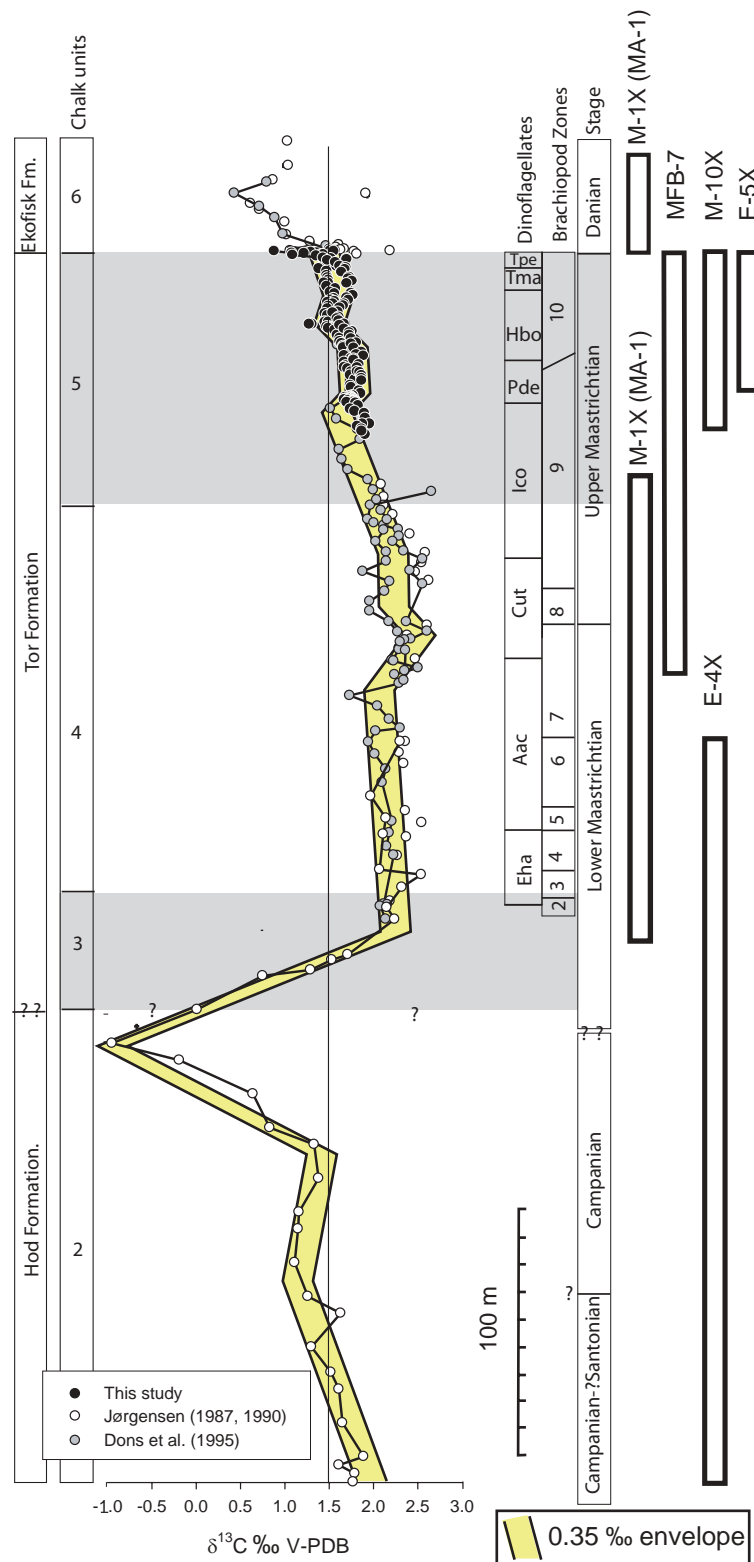


Figure 13: Summary of Maastrichtian  $\delta^{13}\text{C}$  variation in the North Sea. Data presented in Jørgensen (1987, 1990) and Dons *et al.* (1995) have been recalculated to the V-PDB scale (see text). Note that the MA-1 well is a duplicate of the M-1X well and that the two wells are here assumed to have identical stratigraphy. Any offset in isotopic composition between the wells might be related to a slight difference in actual sample depth. Biostratigraphic correlation is based on Bayliss *et al.* (1976) and Schiøler & Wilson (1993). Correlation with brachiopod zones (Surlyk 1984) is according to Schiøler & Wilson (1993). Note that the stratigraphical position of the E-4X well is uncertain. A reference line of 1.5 ‰ is shown.